Future of the human climate niche

Chi Xu (徐驰)[a,1], Timothy A. Kohler[b,c,d,e], Timothy M. Lenton[f], Jens-Christian Svenning[g], and Marten Scheffer[c,h,i,1]

[a]School of Life Sciences, Nanjing University, Nanjing 210023, China; [b]Department of Anthropology, Washington State University, Pullman, WA 99164; [c]Santa Fe Institute, Santa Fe, NM 87501; [d]Crow Canyon Archaeological Center, Cortez, CO 81321; [e]Research Institute for Humanity and Nature, Kyoto 603-8047, Japan; [f]Global Systems Institute, University of Exeter, Exeter, EX4 4QE, United Kingdom; [g]Center for Biodiversity Dynamics in a Changing World, Department of Bioscience, Aarhus University, DK-8000 Aarhus C, Denmark; [h]Wageningen University, NL-6700 AA, Wageningen, The Netherlands; and [i]SARAS (South American Institute for Resilience and Sustainability Studies), 10302 Bella Vista, Maldonado, Uruguay

Contributed by Marten Scheffer, October 27, 2019 (sent for review June 12, 2019; reviewed by Victor Galaz and Luke Kemp)

All species have an environmental niche, and despite technological advances, humans are unlikely to be an exception. Here, we demonstrate that for millennia, human populations have resided in the same narrow part of the climatic envelope available on the globe, characterized by a major mode around ∼11 °C to 15 °C mean annual temperature (MAT). Supporting the fundamental nature of this temperature niche, current production of crops and livestock is largely limited to the same conditions, and the same optimum has been found for agricultural and nonagricultural economic output of countries through analyses of year-to-year variation. We show that in a business-as-usual climate change scenario, the geographical position of this temperature niche is projected to shift more over the coming 50 y than it has moved since 6000 BP. Populations will not simply track the shifting climate, as adaptation in situ may address some of the challenges, and many other factors affect decisions to migrate. Nevertheless, in the absence of migration, one third of the global population is projected to experience a MAT >29 °C currently found in only 0.8% of the Earth's land surface, mostly concentrated in the Sahara. As the potentially most affected regions are among the poorest in the world, where adaptive capacity is low, enhancing human development in those areas should be a priority alongside climate mitigation.

climate | migration | societies

Global warming will affect ecosystems as well as human health, livelihoods, food security, water supply, and economic growth in many ways (1, 2). The impacts are projected to increase steeply with the degree of warming. For instance, warming to 2 °C, compared with 1.5 °C, is estimated to increase the number of people exposed to climate-related risks and poverty by up to several hundred million by 2050. It remains difficult, however, to foresee the human impacts of the complex interplay of mechanisms driven by warming (1, 3). Much of the impact on human well-being will depend on societal responses. There are often options for local adaptations that could ameliorate effects, given enough resources (4). At the same time, while some regions may face declining conditions for human thriving, conditions in other places will improve. Therefore, despite the formidable psychological, social, and political barriers to migration, a change in the geographical distribution of human populations and agricultural production is another likely part of the spontaneous or managed adaptive response of humanity to a changing climate (5). Clearly there is a need to understand the climatic conditions needed for human thriving. Despite a long and turbulent history of studies on the role of climate, and environment at large, on society in geography and beyond (6), causal links have remained difficult to establish, and deterministic claims largely refuted, given the complexities of the relationships in question (7). Rather than reentering the murky waters of environmental determinism (8, 9), here we take a fresh look at this complex and contentious issue. We mine the massive sets of demographic, land use, and climate information that have become available in recent years to ask what the climatic conditions for human life have been across the past millennia, and then examine where those conditions are projected to occur in the future.

Results

Current and Past Human Association to Climate. Our results reveal that today, humans, as well as the production of crops and livestock (Fig. 1 *A*, *D*, and *E*), are concentrated in a strikingly narrow part of the total available climate space (Fig. 1*G*). This is especially true with respect to the mean annual temperature (MAT), where the main mode occurs around ∼11 °C to 15 °C (*SI Appendix*, Fig. S1). By contrast, much of range of precipitation available around that temperature (Fig. 1*G* and *SI Appendix*, Fig. S1) is used, except for the driest end. Soil fertility does not seem to be a major driver of human distribution (Fig. 1*H*), nor can potential productivity be a dominant factor, as net primary productivity shows a quite different geographical distribution (Fig. 1*I*), peaking in tropical rainforests, which have not been the main foci of human settlement.

Strikingly, the apparent conditions for human thriving have remained mostly the same from the mid-Holocene until now (Fig. 1 *A*–*C*). Reconstructions of human distribution and climate are relatively reliable for the past centuries, but uncertainty inevitably increases as we go further back in time. Nonetheless, the two independent sets of available reconstructions we analyzed suggest that as far back as 6000 y BP, humans were concentrated in roughly the same subset of the globally available temperature conditions (Fig. 1*C* and 2*A*), despite people at the time living quite differently from today, mostly in the early phases of

Significance

We show that for thousands of years, humans have concentrated in a surprisingly narrow subset of Earth's available climates, characterized by mean annual temperatures around ∼13 °C. This distribution likely reflects a human temperature niche related to fundamental constraints. We demonstrate that depending on scenarios of population growth and warming, over the coming 50 y, 1 to 3 billion people are projected to be left outside the climate conditions that have served humanity well over the past 6,000 y. Absent climate mitigation or migration, a substantial part of humanity will be exposed to mean annual temperatures warmer than nearly anywhere today.

Author contributions: C.X. and M.S. designed research; C.X., T.A.K., T.M.L., and J.-C.S. performed research; C.X. analyzed data; M.S. wrote the paper; T.A.K. analyzed the archaeological data; and T.A.K., T.M.L., and J.-C.S. commented on all versions of the manuscript and contributed by suggesting novel additional analyses and interpretations.

Reviewers: V.G., Stockholm University; and L.K., University of Cambridge.

The authors declare no competing interest.

[1]To whom correspondence may be addressed. Email: xuchi@nju.edu.cn or marten.scheffer@wur.nl.

This article contains supporting information online at https://www.pnas.org/lookup/suppl/doi:10.1073/pnas.1910114117/-/DCSupplemental.

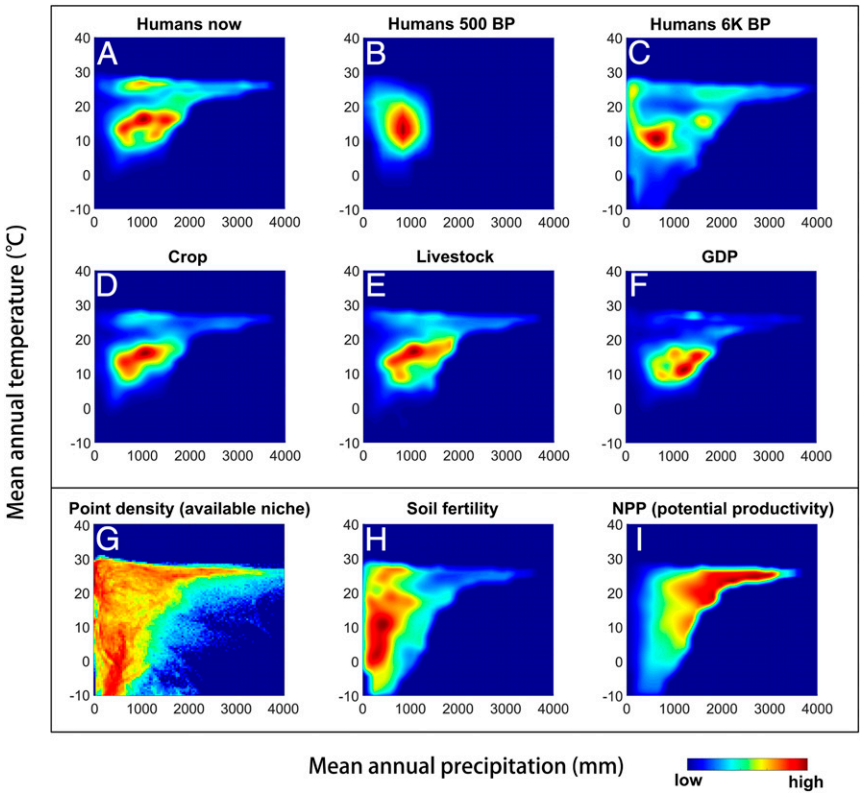

Fig. 1. The realized human climate niche relative to available combinations of MAT and precipitation. Human populations have historically remained concentrated in a narrow subset (*A*–*C*) of the available climatic range (*G*), which is not explained by soil fertility (*H*) or potential primary productivity (*I*). Current production of crops (*D*) and livestock (*E*) are largely congruent with the human distribution, whereas gross domestic product peaks at somewhat lower temperatures. Reconstructions of human populations 500 BP are based on the HYDE database, whereas those for 6 Ky BP are based on ArchaeoGlobe (https://doi.org/10.7910/DVN/CQWUBI, Harvard Dataverse, V4). NPP, net primary productivity. See *SI Appendix, Methods*.

agriculture or as hunter-gatherers. Historical contingency (including path dependence) may play some role in the inertia we observe, especially when it comes to the sites of economic dominance. However, such economic hotspots occur at somewhat colder conditions than the center of the population distributions (Fig. 1*F* vs. Fig. 1*A*), and explaining such patterns of economic dominance requires unraveling the dynamics of historical, cultural, and institutional settings (10–14), which is beyond the scope of this paper.

If we focus at the global distribution of population densities and examine how this codeveloped with climate over time, the precipitation niche turns out to have broadened over the past centuries (Fig. 1*A* vs. Fig. 1*B*), leaving only the driest part of the gradient unoccupied (Fig. 1*A* vs. Fig. 1*G*). In contrast, the human population distribution in relation to MAT has remained largely unaltered (Fig. 2*A*), with a major mode around ∼11 °C to 15 °C accompanied by a smaller secondary mode around ∼20 °C to 25 °C corresponding largely to the Indian Monsoon region (*SI*

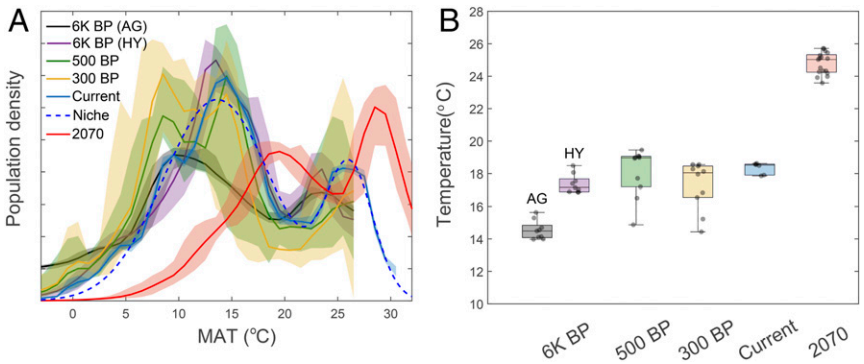

Fig. 2. Change in MAT experienced by humans. (*A*) Current and past human population densities (normalized to sum unity) and modeled human niche (blue dashed curve, a double Gaussian model fitting of current population density) as a function of MAT (°C), contrasted to the projected situation in 2070 (red curve). Bands represent fifth and 95th percentiles of the ensemble of climate and population reconstructions. For the future projection, we take projected populations and climate RCP8.5 and SSP3. (*B*) Mean temperature experienced by a human being in different periods. Boxplots and data points (gray dots) are shown for the ensemble of climate and population reconstructions. Reconstructions of human populations for 6 Ky BP are based on the HYDE (HY) and ArchaeoGLOBE (AG) (with additional processing) databases.

Appendix, Fig. S2). In the remainder, we focus on this realized temperature niche. Results for the combined precipitation–temperature niche are presented for comparison in the *SI Appendix*.

Projected Change. The historical inertia of the human distribution with respect to temperature (Fig. 2) contrasts sharply to the shift projected to be experienced by human populations in the next half century, assuming business-as-usual scenarios for climate (Representative Concentration Pathway 8.5 [RCP8.5]) and population growth (socioeconomic pathway 3 [SSP3]) in the absence of significant migration (Fig. 2*A*, red curve). Absent climate mitigation or human migration, the temperature experienced by an average human is projected to change more in the coming decades than it has over the past six millennia (Fig. 2*B*; for different scenarios of population growth and climate change, see *SI Appendix*, Fig. S3). Compared with the preindustrial situation 300 y BP, the mean human-experienced temperature rise by 2070 will amount to an estimated 7.5 °C, about 2.3 times the mean global temperature rise, a discrepancy that is largely due to the fact that the land will warm much faster than the oceans (2), but also amplified somewhat by the fact that population growth is projected to be predominantly in hotter places (*SI Appendix*, Fig. S3).

One way to get an image of the temperatures projected to be experienced in highly populated areas in 2070 is to look at the regions where comparable conditions are already present in the current climate. Most of the areas that are now close to the historically prevalent ∼13 °C mode will, in 50 y have a MAT ∼20 °C, currently found in regions such as North Africa, parts of Southern China, and Mediterranean regions (*SI Appendix*, Fig. S4). Meanwhile, populations in regions that are currently hot already will grow to represent a major part of the global population (right-hand mode of the red curve in Fig. 2*A*; the role of population growth can be seen in *SI Appendix*, Figs. S5–S7). Those growing populations will experience MATs currently found in very few places. Specifically, 3.5 billion people will be exposed to MAT ≥29.0 °C, a situation found in the present climate only in 0.8% of the global land surface, mostly concentrated in the Sahara, but in 2070 projected to cover 19% of the global land (Fig. 3).

Another way to quantify change is through following the movement of the geographical location of the human temperature niche (Fig. 4 and *SI Appendix*, Figs. S8 and S9). For the RCP8.5 climate change scenario (2), the projected geographical shift of favorable conditions over the coming 50 y is substantial (Fig. 4). Indeed, the movement of the niche on the global map is larger than it has been since 6000 BP (*SI Appendix*, Figs. S8 and S9). These results are robust for different reconstructions of past climate, different approaches to projection of future climate (*SI Appendix*, Fig. S9), and different versions of the ArchaeoGlobe land use reconstructions. Adding precipitation as an additional climate dimension refines the pattern, mostly by excluding deserts, but leaves the overall picture the same (*SI Appendix*, Fig. S10). The bottom line is that over the coming decades, the human climate niche is projected to move to higher latitudes in unprecedented ways (*SI Appendix*, Fig. S11). At the same time, populations are projected to expand predominantly at lower latitudes (*SI Appendix*, Fig. S5), amplifying the mismatch between the expected distribution of humans and the climate.

A Hypothetical Redistribution. As conditions will deteriorate in some regions, but improve in other parts (Fig. 4*C* and *SI Appendix*, Figs. S9 and S10), a logical way of characterizing the potential tension arising from projected climate change is to compute how the future population would in theory have to be redistributed geographically if we are to keep the same distribution relative to temperature (methods and detailed results in the *SI Appendix*, *Material*). Such a calculation suggests that for the RCP8.5 business-as-usual climate scenario, and accounting for expected demographic developments (the SSP3 scenario [15]), ∼3.5 billion people (roughly 30% of the projected global population; *SI Appendix*, Fig. S12) would have to move to other areas if the global population were to stay distributed relative to temperature the same way it has been for the past millennia (*SI Appendix*, Fig. S13). Strong climate mitigation following the RCP2.6 scenario would substantially reduce the geographical shift in the niche of humans and would reduce the theoretically needed movement to ∼1.5 billion people (∼13% of the projected global population; *SI Appendix*, Figs. S12 and S13). Obviously, different scenarios of population growth also have substantial effects on the absolute estimates of potential migration (*SI Appendix*, Table S3). Such niche movement estimates allow quantifying the implications of global warming in nonmonetary terms. For instance, accounting for population growth projected in the SSP3 scenario, each degree of temperature rise above the current baseline roughly corresponds to one billion humans left outside the temperature niche, absent migration (*SI Appendix*, Fig. S14).

Discussion

The transparency of our approach is appealing, but inevitably implies some loss of nuance. For instance, temperature captures only part of the relevant climate (16), and potentially important

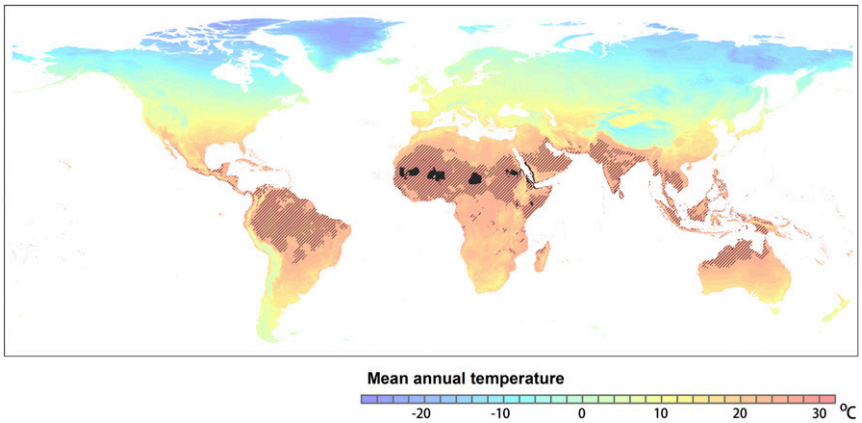

Fig. 3. Expansion of extremely hot regions in a business-as-usual climate scenario. In the current climate, MATs >29 °C are restricted to the small dark areas in the Sahara region. In 2070, such conditions are projected to occur throughout the shaded area following the RCP8.5 scenario. Absent migration, that area would be home to 3.5 billion people in 2070 following the SSP3 scenario of demographic development. Background colors represent the current MATs.

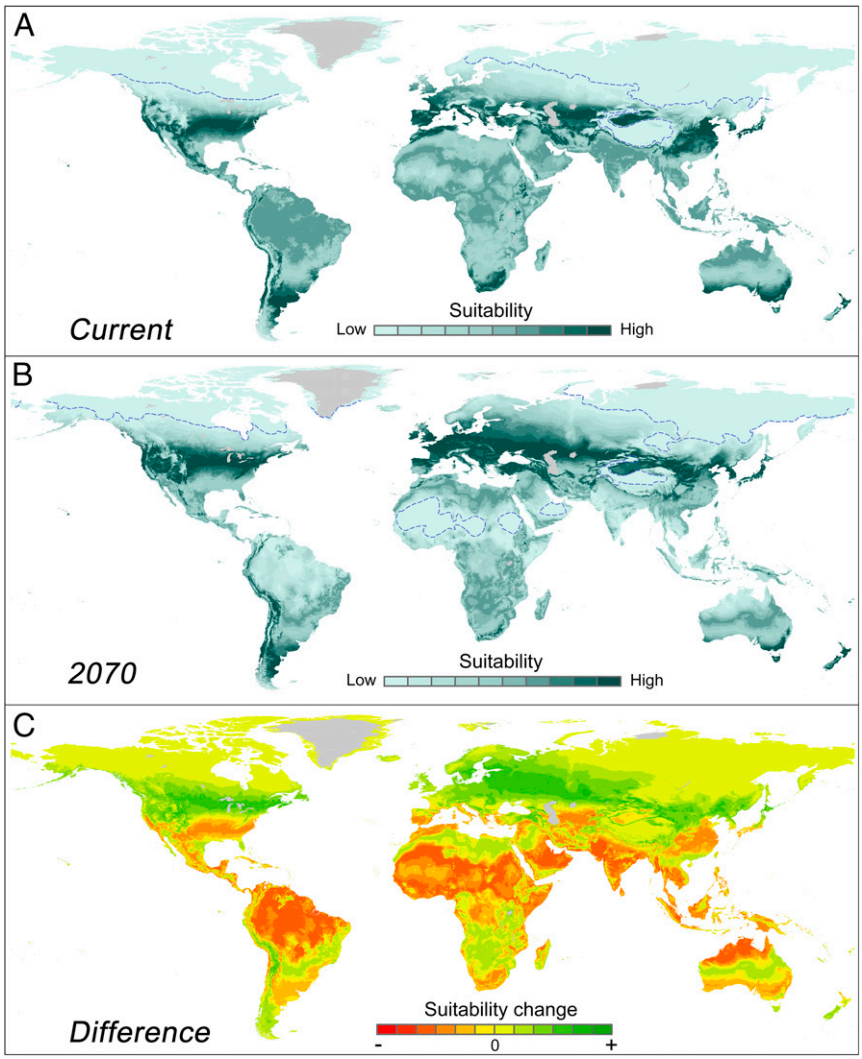

Fig. 4. Projected geographical shift of the human temperature niche. (*Top*) Geographical position of the human temperature niche projected on the current situation (*A*) and the RCP8.5 projected 2070 climate (*B*). Those maps represent relative human distributions (summed to unity) for the imaginary situation that humans would be distributed over temperatures following the stylized double Gaussian model fitted to the modern data (the blue dashed curve in Fig. 2*A*). (*C*) Difference between the maps, visualizing potential source (orange) and sink (green) areas for the coming decades if humans were to be relocated in a way that would maintain this historically stable distribution with respect to temperature. The dashed line in *A* and *B* indicates the 5% percentile of the probability distribution. For an analysis including precipitation effects, see *SI Appendix*, Fig. S10.

drivers of human thriving are linked in complex ways to climate (13). Importantly, while our projection of the geographical shift of the temperature niche is illustrative, it cannot be interpreted as a prediction of migration, as many factors other than climate affect decisions to migrate, and much of the migration demand may potentially be addressed through climate adaptation (5, 17, 18). Those complexities invite reflections on two key questions: First, how could the narrow realized temperature niche be explained? Second, what are the implications in terms of potential future migration in response to geographical displacement of the temperature niche?

The Question of Causality. Why have humans remained concentrated so consistently in the same small part of the potential climate space? The full complex of mechanisms responsible for the patterns is obviously hard to unravel. The constancy of the core distribution of humans over millennia in the face of accumulating innovations is suggestive of a fundamental link to temperature. However, one could argue that the realized niche may merely reflect the ancient needs of agrarian production. Perhaps, people stayed and populations kept expanding in those places, even if the corresponding climate conditions had become irrelevant? Three lines of evidence suggest that this is unlikely, and that instead human thriving remains largely constrained to the observed realized temperature niche for causal reasons.

First, an estimated 50% of the global population depends on smallholder farming (19), and much of the energy input in such systems comes from physical work carried out by farmers, which can be strongly affected by extreme temperatures (20). Second, high temperatures have strong impacts (21–23), affecting not only physical labor capacity but also mood, behavior, and mental health through heat exhaustion and effects on cognitive and psychological performance (20, 24, 25). The third, and perhaps most striking, indication for causality behind the temperature optimum we find is that it coincides with the optimum for economic productivity found in a study of climate-related dynamics in 166 countries (12). To eliminate confounding effects of historical, cultural, and political differences, that study focused on the relation within countries between year-to-year differences in economic productivity and temperature anomalies. The ∼13 °C

optimum in MAT they find holds globally across agricultural and nonagricultural activity in rich and poor countries. Thus, based on an entirely different set of data, that economic study independently points to the same temperature optimum we infer.

Altogether, it seems plausible that the historically stable association between human distribution and temperature reflects a causal link rather than a legacy, contingent on ancient patterns reflecting agrarian needs or still-more-ancient hunter-gatherer preferences. This supports the view that the historically stable and tight relationship of human distribution to MAT represents a human temperature niche reflecting fundamental constraints on human populations.

Migration as a Possible Response to Climate Change. Obviously, our hypothetical redistribution calculations cannot be interpreted in terms of expected migration. First of all, detailed regional studies suggest that migration responds nonlinearly to temperature (18, 26, 27). Thus, migration may speed up only when a critical climate threshold is reached. More generally, migration decisions tend to be avoided and depend on a complex array of factors including adaptation options (5, 17, 18). This implies that realized migration numbers will likely be much lower than suggested by the discrepancy between the expected location of the temperature niche and actual distributions of population, even though we have not considered several drivers that could exacerbate movements, such as extreme weather events or projected sea-level rise, which may by themselves lead to substantial population displacements worldwide (28, 29).

Clearly, projections of the magnitude of climate-driven future migration (including asylum seeking) will remain highly uncertain. Even seemingly straightforward links between climate and recent conflicts and migration waves are contentious. For instance, in the years leading up to the current Syrian exodus, the fertile crescent has likely been experiencing the worst drought in 900 y, making subsistence farming in the countryside extremely hard and driving millions in Syria to the cities, where tensions increased (30). However, as many factors play a role, assessing the relative role of climate in such specific conflict or mass migration events always remains challenging (31, 32). This is not to say that there is no evidence for a causal relationship between conflicts and climate events such as prolonged droughts, both now (33) and in the past (34). In fact, the literature is replete with evidence for ancient episodes of climate-triggered human migration and upheaval (e.g., refs. 34–40). For instance, the coldest phase of the Little Ice Age in Europe (1560 to 1660 AD) has been causally linked to a peak of migration (1580 to 1650 AD) and a European population collapse to a minimum in 1650 AD (41). Earlier, the Late Antique Little Ice Age from 536 to about 660 AD affected most of the Northern Hemisphere, likely contributing to the transformation of the Roman Empire, movements out of the Asian steppe and Arabian Peninsula, spread of Slavic-speaking peoples, and upheavals in China (40). Clearly, lessons from such ancient dynamics cannot be directly extrapolated to modern times. However, while outcomes are context dependent, and confounding social, cultural, and political considerations are always present, a range of analyses suggests that changes of climatic conditions can exert enough stress to trigger migration (5, 17, 18, 42), part of which can take the form of asylum-seeking waves in response to climate-driven conflicts (43).

It thus seems reasonable to assume that at least part of the discrepancy caused by the projected geographical shift in the human temperature niche could be reduced through different forms of migration. However, it remains impossible at this point to foresee the extent of climate-driven redistribution of the human population. Technoeconomic scenarios, political developments, institutional changes, and socioeconomic conditions that affect adaptation options may profoundly affect outcomes in ways that will be worth exploring in further scenario analyses utilizing the different assumptions underlying the SSPs. Also, rising mortality impacts of heat waves on dense populations in already-hot places such as India invite further scrutiny (44). Follow-up work is needed to search for integrative avenues for effective adaptation, as well as defining fundamental limitations to what is possible given available resources.

Outlook. In summary, our results suggest a strong tension between expected future population distributions and the future locations of climate conditions that have served humanity well over the past millennia. So far, the scope for local adaptation has been the dominant focus for analyses of possible responses to a changing climate (4), despite a striking lack of realized adaptation in most regions (12, 13). It is not too late to mitigate climate change and to improve adaptive capacity, especially when it comes to boosting human development in the Global South (45, 46). However, our approach naturally raises the question of what role redistribution of populations may come to play. Migration can have beneficial effects to societies, including a boost to research and innovation (47). However, on larger scales, migration inevitably causes tension, even now, when a relatively modest number of ∼250 million people live outside their countries of birth (48). Looking at the benefits of climate mitigation in terms of avoided potential displacements may be a useful complement to estimates in terms of economic gains and losses.

Methods

We characterized the human climate niche using global gridded datasets for human population as well as a range of social and environmental variables. We used the current population data as well as reconstructed population data available from the History Database of the Global Environment (HYDE 3.1) (49). For early periods, these population data are hindcast from multiple sources. For mid-Holocene, we therefore complement the HYDE data with a reconstruction described in the *SI Appendix* and based on direct estimates from archaeology (50). Details on the sources and preprocessing of data on crop production, livestock distribution, gross domestic product, and past and present MAT and mean annual precipitation (MAP) are also presented in the *SI Appendix*. We plotted heat maps illustrating the past and current human climate niche by calculating the mean population density and other variables within each MAT and MAP combination bin and smoothing the result, excluding bins with sparse data points. We also present running means of relevant variables separately against MAT and MAP in the *SI Appendix*. Uncertainties were characterized as the fifth and 95th percentiles, using different population and climate datasets (*SI Appendix*).

We modeled the realized human temperature niche based on double-Gaussian fitting of the running mean of the current population distribution against MAT (Fig. 2*A*, blue dashed curve). We then projected the modeled niche to the past (6 Ky BP) and future (2070) climate conditions (under different Intergovernmental Panel on Climate Change RCPs) to illustrate the potential geographic shift of human temperature niche under near-future global warming. To test for the robustness against adding precipitation as an additional dimension of human climate niche, we also projected the smoothed human distribution in terms of MAT and MAP to the past and future climates for comparison.

To quantify the projected shift of the human temperature niche, we calculated proportions of summed niche gain or loss. By multiplying the projected world's total population (under different IPCC SSPs) by the proportion of displaced niche, we estimated the numbers that would potentially be displaced if the probability distribution over temperatures were to remain unchanged by 2070.

A detailed description of our materials and methods may be found in the *SI Appendix*, where the reader may also find a broad set of additional results and sensitivity analyses, as well as a Dryad link to the data used and scripts for all computations.

ACKNOWLEDGMENTS. We thank Els Weinans and Shuqing Teng for assistance in data processing and code checking. We also thank Andrew Gillreath-Brown, Henry Wright, Pablo Marquet, and Jennifer Dunne for insightful discussions at the Santa Fe Institute, and Neil Adger for insightful comments on the challenge of foreseeing migration dynamics. This work

was partly funded by the National Key R&D Program of China (Grant 2017YFC0506200 to C.X.), the National Natural Science Foundation of China (Grant 31770512 to C.X.), the European Research Council Advanced Grant and Spinoza award (to M.S.), and a Santa Fe Institute Working Group on The Human Niche (to T.A.K. and M.S.). T.A.K. acknowledges support from the US National Science Foundation Grant SMA-1637171. T.M.L.'s contribution was supported by the Leverhulme Trust (Grant RPG-2018-046) and the Alan Turing Institute, through a Turing Fellowship. J.-C.S. considers this work a contribution to his VILLUM Investigator project "Biodiversity Dynamics in a Changing World" funded by VILLUM FONDEN (Grant 16549).

1. O. Hoegh-Guldberg *et al*., "Impacts of 1.5 °C global warming on natural and human systems" (World Meteorological Organization, Geneva, 2018).
2. IPCC, Climate change 2014: Synthesis report. Contribution of working groups I, II, and III to the fifth assessment report of the intergovernmental panel on climate change" (IPCC, Geneva 2014).
3. P. J. First, "Global warming of 1.5 C An IPCC special report on the impacts of global warming of 1.5 C above pre-industrial levels and related global greenhouse gas emission pathways, in the context of strengthening the global response to the threat of climate change, sustainable development, and efforts to eradicate poverty" (World Meteorological Organization, Geneva, 2018).
4. J. Elliott *et al*., Constraints and potentials of future irrigation water availability on agricultural production under climate change. *Proc. Natl. Acad. Sci. U.S.A.* **111**, 3239–3244 (2014).
5. R. McLeman, B. Smit, Migration as an adaptation to climate change. *Clim. Change* **76**, 31–53 (2006).
6. H. Stephen, *Empire: A Very Short Introduction* (Oxford University Press, 2002).
7. K. W. Butzer, Collapse, environment, and society. *Proc. Natl. Acad. Sci. U.S.A.* **109**, 3632–3639 (2012).
8. D. N. Livingstone, Changing climate, human evolution, and the revival of environmental determinism. *Bull. Hist. Med.* **86**, 564–595 (2012).
9. E. Huntington, *Climate and Civilization* (Harper & Bros., 1915).
10. D. Acemoglu, S. Johnson, J. A. Robinson, "Institutions as a fundamental cause of long-run growth" in *Handbook of Economic Growth*, P. Aghion, S. Durlauf, Eds. (Elsevier, 2005) vol. 1, pp. 385–472.
11. D. Acemoglu, J. A. Robinson, *Why Nations Fail The Origins of Power, Prosperity and Poverty* (Profile Books, 2013), p. 464.
12. M. Burke, S. M. Hsiang, E. Miguel, Global non-linear effect of temperature on economic production. *Nature* **527**, 235–239 (2015).
13. T. A. Carleton, S. M. Hsiang, Social and economic impacts of climate. *Science* **353**, aad9837 (2016).
14. J. M. Diamond, *Guns, Germs, and Steel: The Fates of Human Societies* (W. W. Norton & Company, New York, 1997).
15. B. C. O'Neill *et al*., A new scenario framework for climate change research: The concept of shared socioeconomic pathways. *Clim. Change* **122**, 387–400 (2014).
16. C. Small, J. Cohen, Continental physiography, climate, and the global distribution of human population. *Curr. Anthropol.* **45**, 269–277 (2004).
17. R. Reuveny, Climate change-induced migration and violent conflict. *Polit. Geogr.* **26**, 656–673 (2007).
18. V. Mueller, C. Gray, K. Kosec, Heat stress increases long-term human migration in rural Pakistan. *Nat. Clim. Chang.* **4**, 182–185 (2014).
19. S. K. Lowder, J. Skoet, T. Raney, The number, size, and distribution of farms, smallholder farms, and family farms worldwide. *World Dev.* **87**, 16–29 (2016).
20. T. Kjellstrom *et al*., Heat, human performance, and occupational health: A key issue for the assessment of global climate change impacts. *Annu. Rev. Public Health* **37**, 97–112 (2016).
21. C. Mora *et al*., Global risk of deadly heat. *Nat. Clim. Chang.* **7**, 501 (2017).
22. K. K. Murari, S. Ghosh, A. Patwardhan, E. Daly, K. Salvi, Intensification of future severe heat waves in India and their effect on heat stress and mortality. *Reg. Environ. Change* **15**, 569–579 (2015).
23. S. Russo, J. Sillmann, A. Sterl, Humid heat waves at different warming levels. *Sci. Rep.* **7**, 7477 (2017).
24. L. Taylor, S. L. Watkins, H. Marshall, B. J. Dascombe, J. Foster, The impact of different environmental conditions on cognitive function: A focused review. *Front. Physiol.* **6**, 372 (2016).
25. N. Gaoua, J. Grantham, S. Racinais, F. El Massioui, Sensory displeasure reduces complex cognitive performance in the heat. *J. Environ. Psychol.* **32**, 158–163 (2012).
26. R. McLeman, Thresholds in climate migration. *Popul. Environ.* **39**, 319–338 (2018).
27. P. Bohra-Mishra, M. Oppenheimer, S. M. Hsiang, Nonlinear permanent migration response to climatic variations but minimal response to disasters. *Proc. Natl. Acad. Sci. U.S.A.* **111**, 9780–9785 (2014).
28. R. J. Nicholls *et al*., Sea-level rise and its possible impacts given a 'beyond 4 C world'in the twenty-first century. *Philos. Trans. R. Soc. A* **369**, 161–181 (2011).
29. B. Neumann, A. T. Vafeidis, J. Zimmermann, R. J. Nicholls, Future coastal population growth and exposure to sea-level rise and coastal floodingA global assessment. *PLoS One* **10**, e0118571 (2015).
30. C. P. Kelley, S. Mohtadi, M. A. Cane, R. Seager, Y. Kushnir, Climate change in the Fertile Crescent and implications of the recent Syrian drought. *Proc. Natl. Acad. Sci. U.S.A.* **112**, 3241–3246 (2015).
31. M. Brzoska, C. Fröhlich, Climate change, migration and violent conflict: Vulnerabilities, pathways and adaptation strategies. *Migr. Dev.* **5**, 190–210 (2016).
32. J. Selby, O. S. Dahi, C. Fröhlich, M. Hulme, Climate change and the Syrian civil war revisited. *Polit. Geogr.* **60**, 232–244 (2017).
33. C.-F. Schleussner, J. F. Donges, R. V. Donner, H. J. Schellnhuber, Armed-conflict risks enhanced by climate-related disasters in ethnically fractionalized countries. *Proc. Natl. Acad. Sci. U.S.A.* **113**, 9216–9221 (2016).
34. T. A. Kohler, S. G. Ortman, K. E. Grundtisch, C. M. Fitzpatrick, S. M. Cole, The better angels of their nature: Declining violence through time among prehispanic farmers of the Pueblo Southwest. *Am. Antiq.* **79**, 444–464 (2014).
35. T. D. Dillehay, Archaeology. Climate and human migrations. *Science* **298**, 764–765 (2002).
36. W. J. D'Andrea, Y. Huang, S. C. Fritz, N. J. Anderson, Abrupt Holocene climate change as an important factor for human migration in West Greenland. *Proc. Natl. Acad. Sci. U.S.A.* **108**, 9765–9769 (2011).
37. L. S. Cordell, C. R. Van West, J. S. Dean, D. A. Muenchrath, Mesa Verde settlement history and relocation: Climate change, social networks, and Ancestral Pueblo migration. *Kiva* **72**, 379–405 (2007).
38. A. Timmermann, T. Friedrich, Late Pleistocene climate drivers of early human migration. *Nature* **538**, 92–95 (2016).
39. P. B. deMenocal, C. Stringer, Human migration: Climate and the peopling of the world. *Nature* **538**, 49–50 (2016).
40. U. Büntgen *et al*., Cooling and societal change during the Late Antique Little Ice Age from 536 to around 660 AD. *Nat. Geosci.* **9**, 231 (2016).
41. D. D. Zhang *et al*., The causality analysis of climate change and large-scale human crisis. *Proc. Natl. Acad. Sci. U.S.A.* **108**, 17296–17301 (2011).
42. I. Chort, M. de la Rupelle, Determinants of Mexico-US outward and return migration flows: A state-level panel data analysis. *Demography* **53**, 1453–1476 (2016).
43. G. J. Abel, M. Brottrager, J. C. Cuaresma, R. Muttarak, Climate, conflict and forced migration. *Glob. Environ. Change* **54**, 239–249 (2019).
44. O. Mazdiyasni *et al*., Increasing probability of mortality during Indian heat waves. *Sci. Adv.* **3**, e1700066 (2017).
45. W. Lutz, R. Muttarak, Forecasting societies' adaptive capacities through a demographic metabolism model. *Nat. Clim. Chang.* **7**, 177–184 (2017).
46. W. Lutz, R. Muttarak, E. Striessnig, Environment and development. Universal education is key to enhanced climate adaptation. *Science* **346**, 1061–1062 (2014).
47. G. Scellato, C. Franzoni, P. Stephan, A mobility boost for research. *Science* **356**, 694 (2017).
48. E. Culotta, People on the move. *Science* **356**, 676–677 (2017).
49. K. Klein Goldewijk, A. Beusen, G. Van Drecht, M. De Vos, The HYDE 3.1 spatially explicit database of human-induced global land-use change over the past 12,000 years. *Glob. Ecol. Biogeogr.* **20**, 73–86 (2011).
50. L. Stephens *et al*., Archaeological assessment reveals Earth's early transformation through land use. *Science* **365**, 897–902 (2019).

Supplementary Materials

Future of the human climate niche

Chi Xu [1,*], *Timothy A. Kohler* [2,3,4,5], *Timothy M. Lenton* [6], *Jens-Christian Svenning* [7], *and Marten Scheffer* [3,8,9,*]

1. *School of Life Sciences, Nanjing University, China*
2. *Department of Anthropology, Washington State University, Pullman, USA*
3. *Santa Fe Institute, Santa Fe, USA*
4. *Crow Canyon Archaeological Center, Cortez, USA*
5. *Research Institute for Humanity and Nature, Kyoto, Japan*
6. *Global Systems Institute, University of Exeter, Exeter, UK*
7. *Center for Biodiversity Dynamics in a Changing World, Department of Bioscience, Aarhus University, Aarhus C, Denmark*
8. *Wageningen University, The Netherlands*
9. *SARAS Institute, Uruguay*

** Corresponding authors: marten.scheffer@wur.nl and xuchi@nju.edu.cn*

www.pnas.org/cgi/doi/10.1073/pnas.1910114117

Materials and Methods

Data sources and pre-processing

We conducted systematic analyses to characterize the human climate niche using global gridded datasets for human population as well as a range of social and environmental variables. We used the current (2015 CE) population data (10-km spatial resolution) available from the History Database of the Global Environment (HYDE 3.1, downloaded from http://themasites.pbl.nl/tridion/en/themasites/hyde/) [1]. Reconstructed population data for mid-Holocene (~6Ky BP), 500y BP and 300y BP are also available from the HYDE 3.1 database. For early periods these population data are hindcast from multiple sources. Empirical archaeological evaluation of these hindcasts is only beginning; non-spatially explicit comparisons between taphonomically corrected frequency distributions of calibrated ^{14}C dates and the HYDE 3.1 estimates show many similar features through time for North America and Australia [2]. The HYDE 3.1 population distributions for 1000 CE are considered sufficiently accurate for the rice cultivation areas of Asia to serve as a starting point for estimating earlier and later methane production from rice cultivation and livestock pastoralism [3].

For mid-Holocene, we also reconstructed the distribution of population density based on direct estimates from archaeology, drawing on the ArchaeoGlobe database, for comparison with the hindcasted HYDE data. The ArchaeoGlobe public data v2.0 [4] and their regions [5] were downloaded from Harvard Dataverse (we also repeated all analyses using the ArchaeoGlobe public data v3.0 that was updated after submitting the manuscript, and the results are highly robust to the updated data). The ArchaeoGlobe public dataset contains estimates of how widespread various adaptation types were in each of 146 regions in each of 10 periods from 10Ky BP to 1850 CE, crowd-sourced by invitation from archaeologists with established expertise in each region. A new dataset was created with the modal commonality categories (possible values are none, minimal [<1%], common [1-20%], and widespread [>20%]) for each of four adaptation types (foraging/hunting/gathering/fishing [FHGH], extensive agriculture [EA], intensive agriculture [IA], and pastoralism [P]) for each region, for the 6Ky BP period. Thirteen regions with no density estimates were coded as missing values. On average there were 4.5 different coders (i.e., estimates of commonality) for each region with non-missing values.

To obtain density estimates for FHGH populations we used effective temperatures estimated for 6Ky BP generated from simulations with the downscaled Global Climate Models from the IPPC Fifth Assessment Report (CMIP5), assigning each ArchaeoGlobe region to one of seven climate classes as defined in Binford (2001 Table 7.02) [6]. We then computed the mean population densities for FHGH populations for each climate zone from Binford's tabulation, and divided these by 100 to get densities/km^2, as follows:

1. polar, .053
2. boreal, .123
3. cool temperate, .421
4. warm temperate, .262
5. subtropical, .374
6. tropical, .374
7. equatorial, .345

Population density estimates for other adaptation types were not indexed by climate zone, and were taken from Hassan (1981: Figure 4.1) [7] as follows: EA (Hassan's "early dry farming") and P, 5 persons/km^2; and IA, 15 persons/km^2.

Finally, we considered the codes "widespread" to equal 30%, "common" to equal 10%, "minimal" to equal 1%, and "none" to equal 0%. For each region, these numbers were summed and divided by 100 to obtain the raising factor necessary to make these sum to 1. Then regionally and adaptationally appropriate population densities could be computed using the raised proportions to admix the "pure" population densities. For example, for a region in the cool temperate zone in which FHGF and EA are both "widespread" and IA and P are absent, each 30% gets raised to 50% and the admixed population density for that zone is computed as (0.5 × 0.421) + (0.5 × 5) = 2.71.

The projected population data (~15-km resolution) for the time period 2070 under 5 Shared Socioeconomic Pathways (i.e., SSP1-5) were downloaded from the website of the Climate and Global Dynamics Laboratory of the National Center for Atmospheric Research (http://www.cgd.ucar.edu/iam/modeling/spatial-population-scenarios.html) [8].

We examined actual crop production, livestock distribution, and gross domestic product (GDP) to comprehensively characterize human niches in terms of socioeconomic dimensions for the current conditions. The GDP data for the year 2015 are available from a 1-km resolution global GDP dataset compiled by Kummu and Guillaume [9] (downloaded from https://datadryad.org/resource/doi:10.5061/dryad.dk1j0/9 [10]). The actual total crop production data for the year 2000 (10-km resolution) are available from the Global Agro-ecological Zones Data Portal (GAEZ version 3.0, http://gaez.fao.org/) [11]. The livestock data (1-km resolution) for the year 2006 are available from the FAO Gridded Livestock of the World version 2.0 (downloaded from https://livestock.geo-wiki.org/Application/index.php) [12]. We converted the data for different livestock species (including cattle, pig, goat, sheep, duck and chicken) to the standard livestock unit (LSU) using the coefficients from Eurostats (http://ec.europa.eu/eurostat/statistics-explained/index.php/Glossary:Livestock_unit_(LSU)).

The mean annual temperature (MAT) and mean annual precipitation (MAP) data (~1-km resolution) for the mid-Holocene (6Ky BP), current and future (2070) conditions are available from the WorldClim dataset version 1.4 (http://www.worldclim.org) [13]. The climate data for the current conditions (representative of 1960-1990) were generated from interpolated weather station data. The climate data (Table S1) for 6Ky BP and 2070 (averaged for the period 2061-2080) were generated from simulations with the downscaled Global Climate Models (GCMs) from the IPPC Fifth Assessment Report (CMIP5). For the time period 2070 we take into account three Representative Concentration Pathways (i.e., RCP2.6, RCP4.5 and RCP8.5; RCP6.0 was not included in this study because it is close to RCP4.5 by the year 2070) that are used for characterizing different scenarios of greenhouse gas concentration trajectories adopted by the IPCC for its fifth Assessment Report (AR5).

The climate data for 500y BP and 300y BP were reconstructed from the near-surface air temperature (tas) and precipitation (pr) variables in the "past1000" experiment as part of the Palaeoclimate Modeling

Intercomparison Project 3 (PMIP3) [14]. The simulation models used are shown in Table S2 (see https://data.giss.nasa.gov/modelE/ar5/ for model details).

The mean annual NPP data (~1-km resolution) during 2000-2015 retrieved from the MODIS MOD17A3 product are available from the online Data Pool (https://lpdaac.usgs.gov/dataset_discovery/modis/modis_products_table/mod17a3), courtesy of the NASA EOSDIS Land Processes Distributed Active Archive Center (LP DAAC), USGS/Earth Resources Observation and Science (EROS) Center, Sioux Falls, South Dakota. Total exchangeable bases (the sum of HCl-soluble bases including Ca^{2+}, Mg^{2+}, K^{+} and Na^{+}) were used as an indicator of soil fertility [15]. The soil data (1-km resolution) are available from the Harmonized World Soil Database version 1.2 (http://www.fao.org/soils-portal/soil-survey/soil-maps-and-databases/harmonized-world-soil-database-v12) [16].

All spatial data were resampled to a consistent spatial resolution of 0.083 decimal degree (~10 km) for subsequent analyses.

Data analyses

We plotted heat maps in the MAP-MAT space to illustrate the hotspots of human distribution for the past and current conditions (Fig. 1A-C). The heat maps were produced by calculating the mean population density within each bin (sized of 40 mm MAP × 0.5 °C MAT for the current condition in Fig. 1A and 6Ky BP in Fig. 1C; a coarser bin size of ~130 mm MAP × ~1.5 °C MAT was used for Fig. 1B to avoid seriously discontinuous distribution of the data points caused by the coarse resolution of the climate data for 500y BP) in the state space, and then the result was smoothed by a low-pass filter with 5 × 5 bins. To account for potential bias induced by sparse sampling, we excluded the bins with sparse data points (i.e. data point densities lower than 1st percentile, <~30 data points). Using the same approach, we also plotted the current distributions for crop production, livestock unit, GDP, soil fertility and NPP, respectively (Fig. 2D-F, H-I). Point density in each bin (before smoothing) in the climate state space was shown in Fig. 2G (for illustration, point density was log-transformed due to its highly skewed distribution).

We plotted the running mean of population density, crop production, livestock unit and GDP against MAT (with a bin size of 2 °C) and MAP (with a bin size of 200 mm) for the current condition (Fig. S1). We then compared the running mean of population density (normalize to sum unity) against MAT for the past, current and future conditions (Fig. 2A, Fig. S6). To account for uncertainties of reconstructed past climate and projected future climate conditions, we calculated the 5th and 95th percentiles of the running mean curves using all ensemble data from the climate models. For the current condition, we also conducted an uncertainty analysis by including another population dataset of 2015 (The Gridded Population of the World, Version 4: Population Density Adjusted to Match 2015 Revision of UN WPP Country Totals [17]), and two other climate datasets (the Climate Research Unit's High-resolution gridded datasets v4.02 [18] and the TerraClimate dataset [19]) for MAT and MAP representative of 1960-1990. The 5th and 95th percentiles were also calculated for the running mean curves generated from all combinations of climate and population datasets (2 population datasets × 3 climate datasets, note that in this particular case with sparse data, the 5th-95th percentile envelope is equivalent to the minimum-maximum envelope).

We modeled the realized human climate niche based on double-Gaussian fitting of the running mean of the current population distribution against MAT (Fig. 2A, blue dashed curve). We then projected the modelled niche to the past (6Ky BP) and future (2070, under different RCPs) climate conditions to illustrate the geographic shift of human climate niche over time (Fig. 3, Figs. S8-S10). To test for the robustness of adding precipitation as an additional dimension of human climate niche, we also projected the smoothed human distribution in terms of MAT and MAP (Fig. 1A) to the past and future climates (Fig. S10).

To quantify the geographic shift of human climate niche in terms of MAT, we calculated percentage proportion of summed niche gain or loss (Fig. S12). By multiplying the projected world's total population by the proportion of displaced human niche, we estimated the number of people who would need to be displaced if the climate niche remained unchanged by the year 2070 in different demographic (SSPs) and climate (RCPs) scenarios (Fig. S13, Table S3). Using this result we also estimated the number of potentially displaced people per degree warming (on average) relative to the pre-industrial period in different SSPs based on the warming trajectories [20] of RCP2.6 and RCP8.5 (Fig. S14). We also calculated the mean geographic latitude of the human climate niche for different time periods to demonstrate the shift of niche towards high latitudes in the future ~50 years (Fig. S11).

For the different time periods, we quantified mean temperature experienced by an average human as a function of global mean of MAT weighted by population density. For 2070, when absent of migration, we considered different scenarios of climate change (RCP2.6, RCP4.5 and RCP8.5) and population growth (zero growth relative to the 2015 condition, and SSP1-5). We included different climate models (Table S1, S2) to account for uncertainties of climate change.

The scripts for all computations and the data used in the analyses are deposited in Dryad (https://doi.org/10.5061/dryad.fj6q573q7).

Table S1. The downscaled 1-km Global Climate Models used (×) for calculating climate data for the time periods 2070 and mid-Holocene. See the WorldClim website (http://www.worldclim.org/) for details.

Model	code	2070			Mid Holocene (6Ky BP)
		RCP2.6	RCP4.5	RCP8.5	
ACCESS1-0	AC	-	×	×	-
BCC-CSM1-1	BC	-	×	×	×
CCSM4	CC	×	×	×	×
CESM1-CAM5-1-FV2	CE	-	×	-	-
CNRM-CM5	CN	×	×	×	×
GFDL-CM3	GF	×	×	×	-
GFDL-ESM2G	GD	×	×	-	-
GISS-E2-R	GS	×	×	×	-
HadGEM2-AO	HD	×	×	×	-
HadGEM2-CC	HG	-	×	×	×
HadGEM2-ES	HE	×	×	×	×
INMCM4	IN	-	×	×	-
IPSL-CM5A-LR	IP	×	×	×	×
MIROC-ESM-CHEM	MI	×	×	×	-
MIROC-ESM	MR	×	×	×	×
MIROC5	MC	-	×	×	-
MPI-ESM-LR	MP	×	×	×	-
MRI-CGCM3	MG	×	×	×	×
NorESM1-M	NO	×	×	×	-
MPI-ESM-P	ME	-	-	-	×

Table S2. The Global Climate Models used for calculating climate data for the time periods 500y BP and 300y BP. To account for volcanic forcing, the ensemble members for GISS-E2-R were r1i1p121, r1i1p1221, r1i1p124, r1i1p125, r1i1p127, and r1i1p128, with r1i1p1 for all other models. See the model website (https://data.giss.nasa.gov/modelE/ar5/) for details.

Model	Ensemble member	Original spatial resolution (degree)	Reference
CSIRO-Mk3L-1-2	r1i1p1	5.625 ×3.18	[21]
GISS-E2-R	r1i1p121, r1i1p1221, r1i1p124, r1i1p125, r1i1p127, r1i1p128	2.5 × 2	[22]
HadCM3	r1i1p1	3.75 × 2.5	[23]
IPSL-CM5A-LR	r1i1p1	3.75 × 1.89	[24]
MPI-ESM-P	r1i1p1	1.875 × 1.86	[25]

Figure S1. Running mean of population density (HYDE 3.1), crop production, livestock, and GDP against mean annual temperature (MAT) and mean annual precipitation (MAP) from the WorldClim dataset for the current condition. All data were normalized to sum unity. The consistent optima of the socioeconomic variables mark a global realized human climate niche.

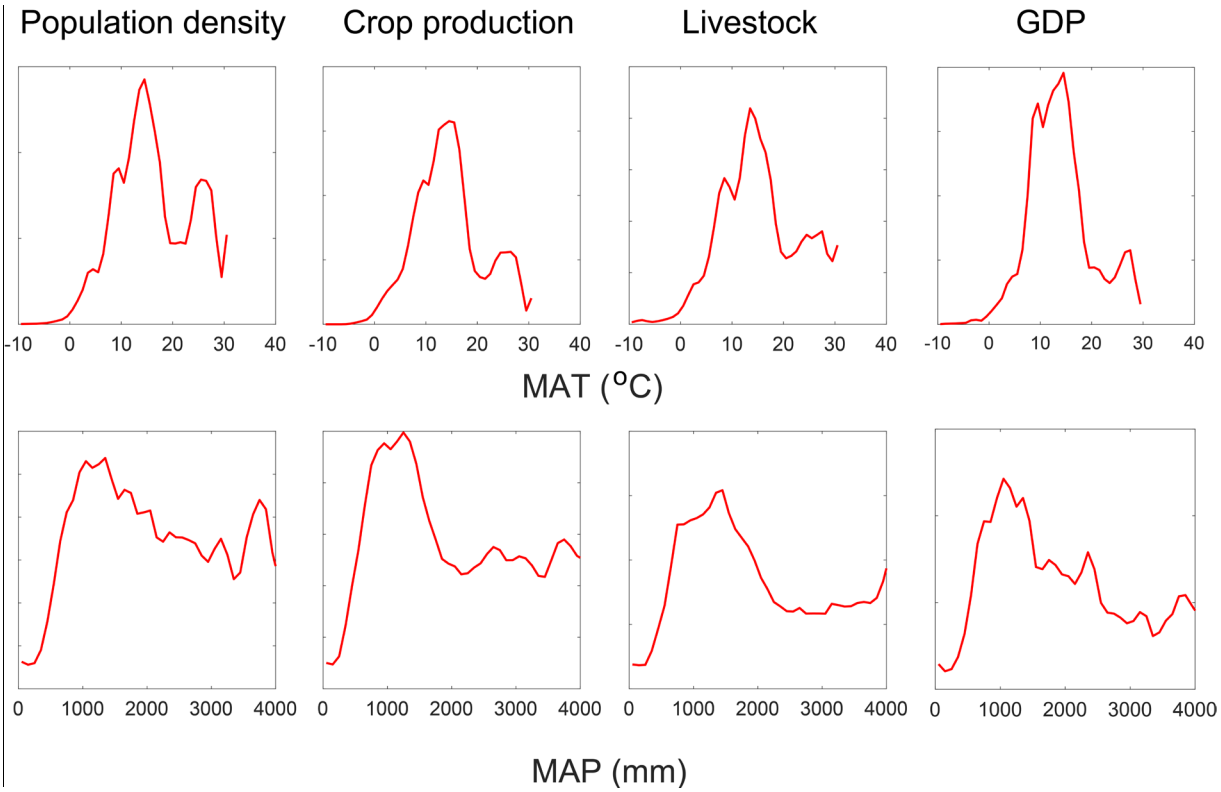

Figure S2. The exclusion of Indian monsoon region (right column) in comparison to all global areas (left column) reveals that the population density mode around ~20-25 °C corresponds largely to the Indian monsoon region. Upper row: running mean of population density (solid curves with bands representing the minimum-maximum envelope) and fitted double Gaussian niche (dashed curves) using the method in Fig. 2; lower row: hot spots of population density in the MAT-MAP space using the method for Fig. 1 (the red-yellow-blue gradient represents population density from high to low).

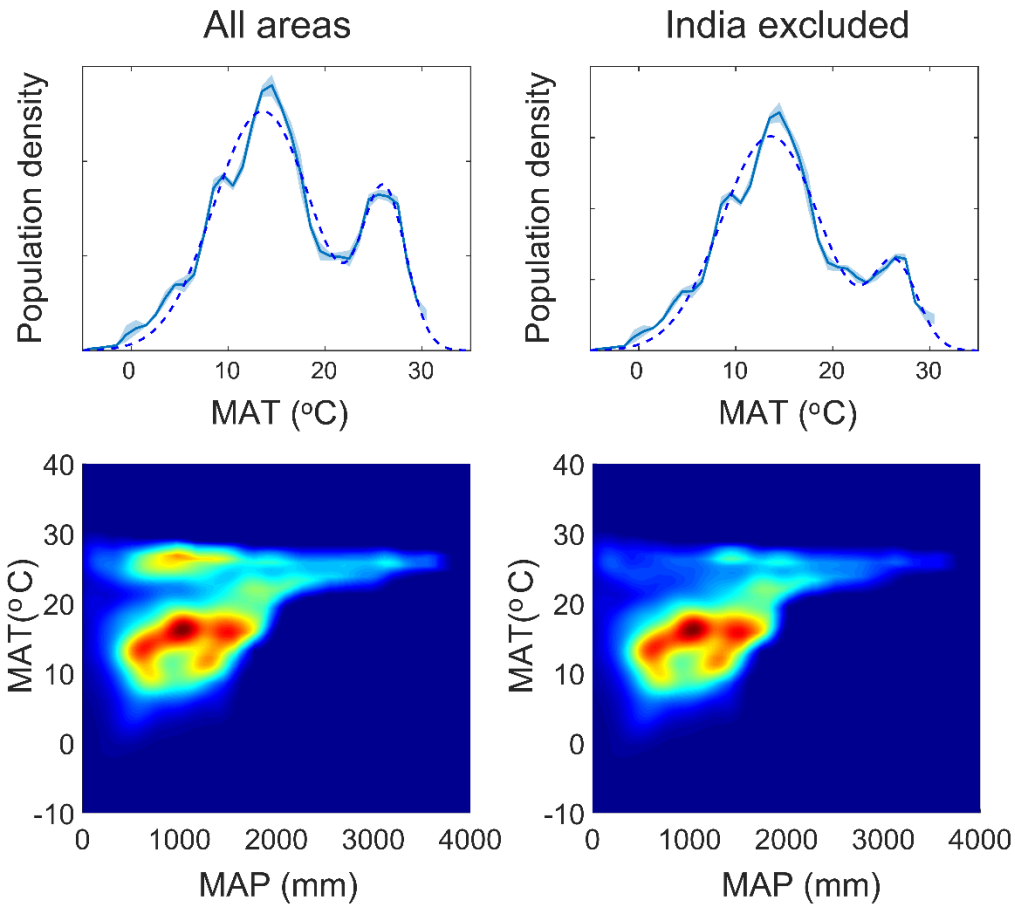

Figure S3. Mean temperature experienced by a human being in different periods. Boxplots and data points (gray dots) are shown for the ensemble of climate and population reconstructions. Different scenarios of climate (RCP2.6, RCP4.5 and RCP8.5) and population growth (zero growth, and SSP1-5) were considered. Reconstructed population data based on the HYDE 3.1 (HY) and ArchaeoGlobe (AG) database were used for 6Ky BP.

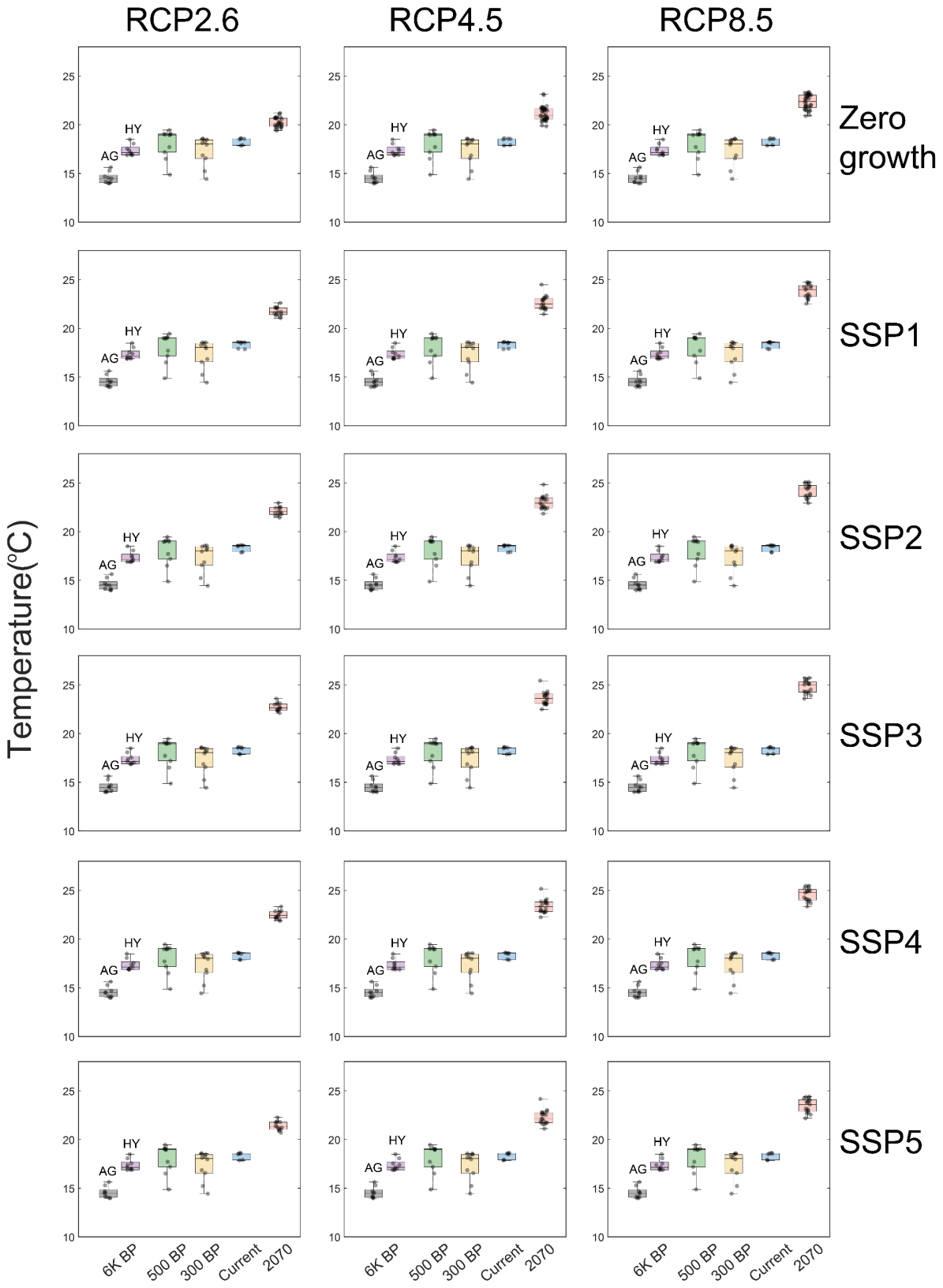

Figure S4. Mean annual temperatures between 17 and 22 °C represent a mode of the projected human temperature niche in 2070 following the RCP 8.5 and SSP3 scenarios (the left-hand mode of the red curve in Fig. S7). In the current climate, such conditions are distributed in the gray areas, but are projected to change to the shaded areas in 2070 (RCP 8.5). Background colors represent the current mean annual temperatures.

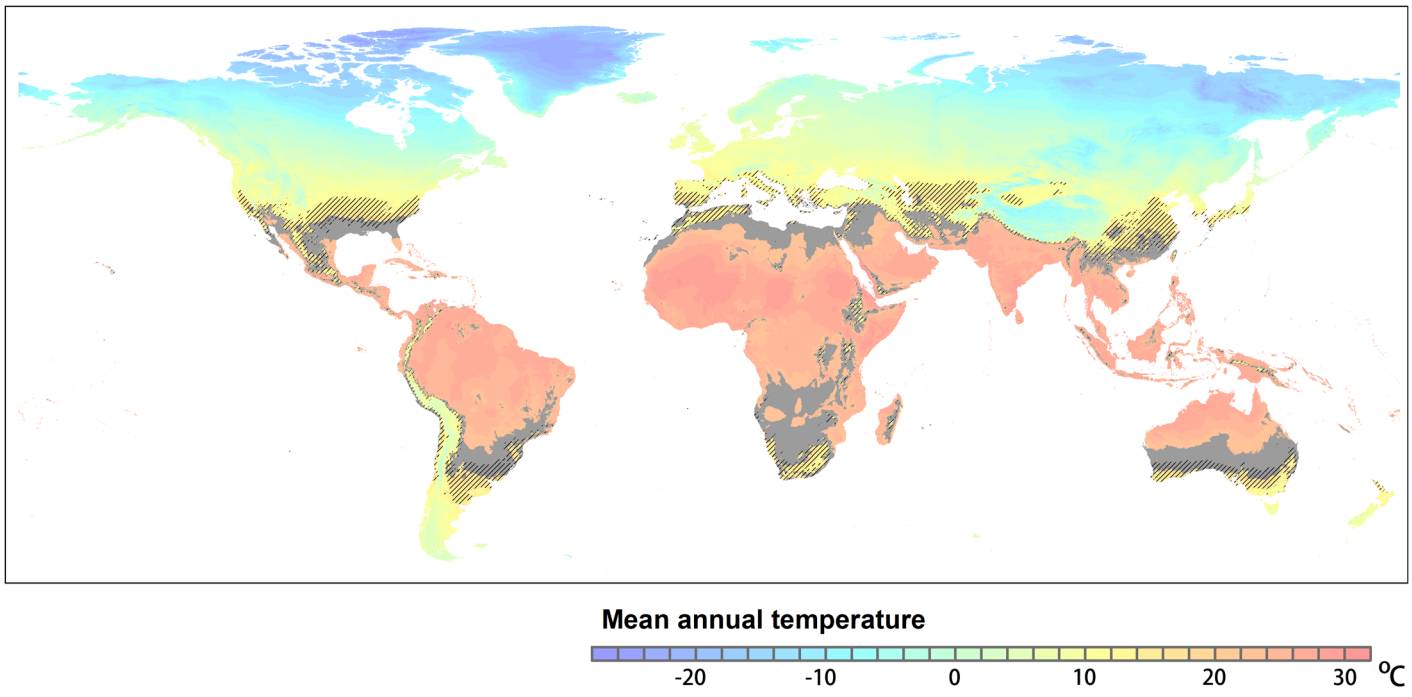

Figure S5. Global distribution of human population densities (A) as compared to the projected population distribution in 2070 following the SSP3 scenario (B). Note differences in upper bound of largest bin.

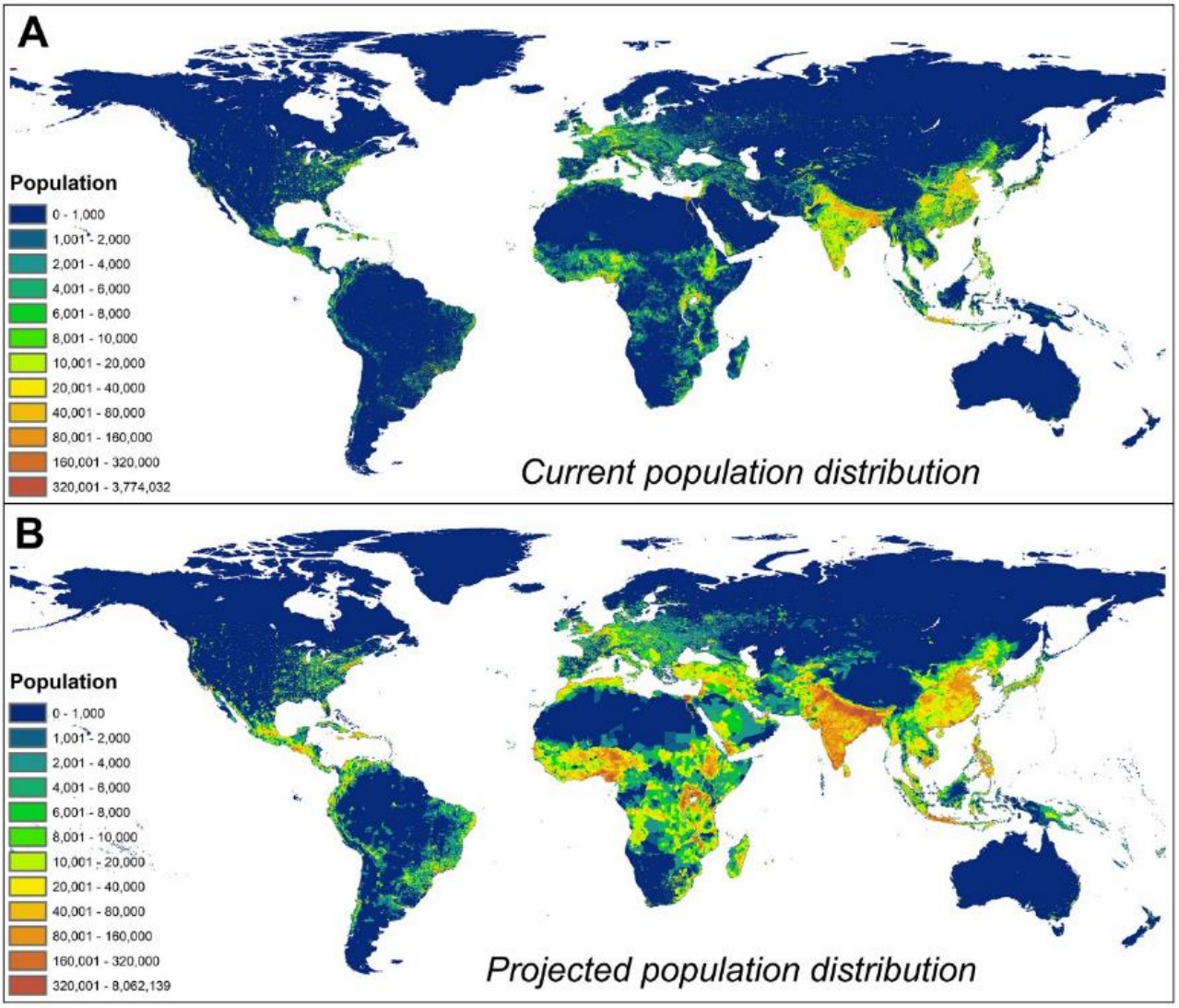

Figure S6. Current and past human population densities (normalized to sum unity) as a function of mean annual temperature (MAT), contrasted to the projected situation in 2070 (red). Different scenarios of climate (RCP2.6, RCP4.5 and RCP8.5) and population growth (zero growth, and SSP1-5) were considered. Bands represent 5th and 95th percentiles of the ensemble of climate and population reconstructions. Reconstructed population data based on the HYDE 3.1 (HY) and ArchaeoGlobe (AG) database were used for 6Ky BP.

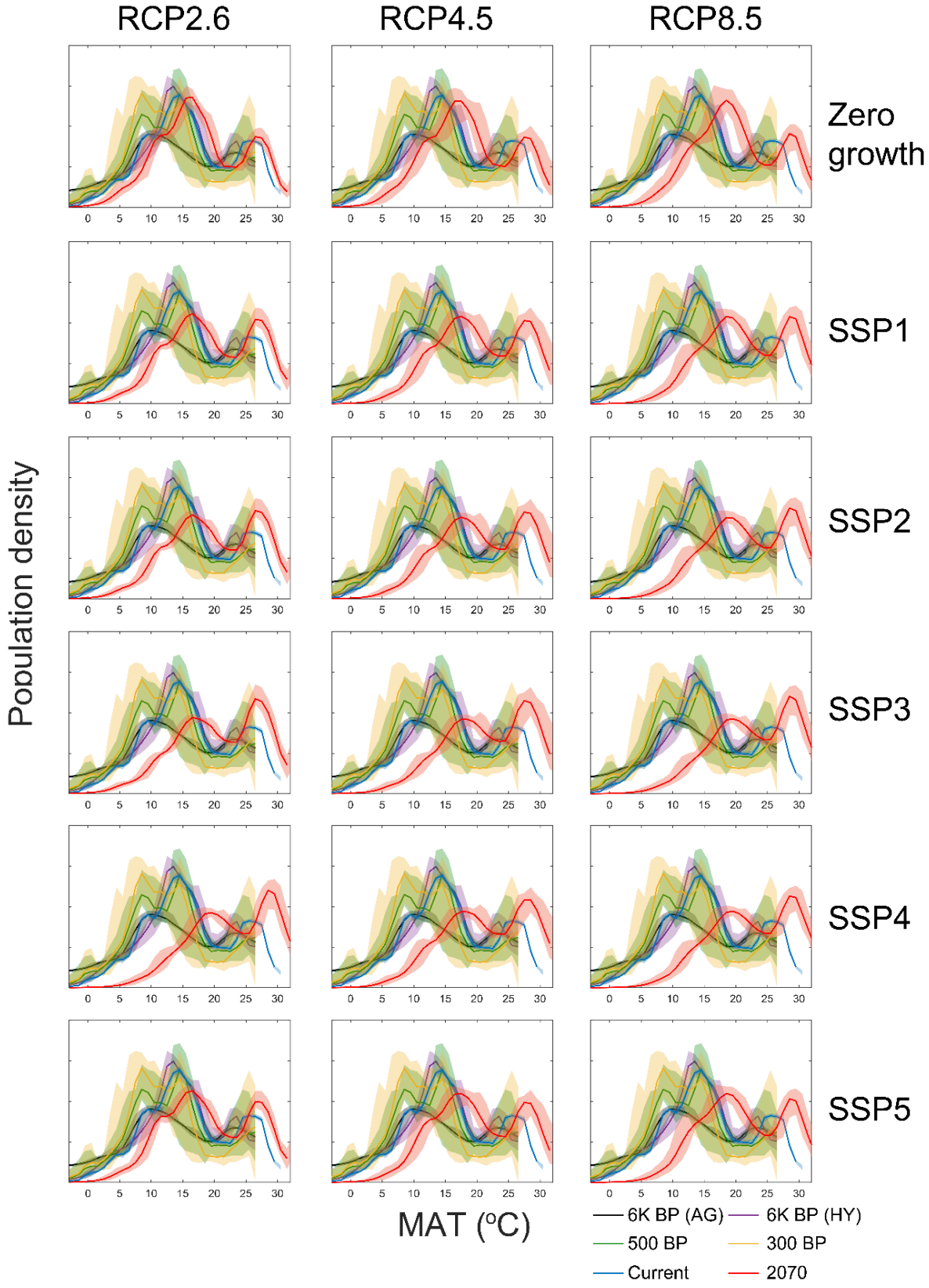

Figure S7. Past and current human niche (fitted by double Gaussian models) in terms of mean annual temperature (MAT), contrasted to the projected situation in 2070 (red). Bands represent 5th and 95th percentiles of the ensemble of climate and population reconstructions. Different scenarios of climate (RCP2.6, RCP4.5 and RCP8.5) and population growth (zero growth, and SSP1-5) were considered. Bands represent 5th and 95th percentiles of the ensemble of climate and population reconstructions. Reconstructed population data based on the HYDE 3.1 (HY) and ArchaeoGlobe (AG) database were used for 6Ky BP.

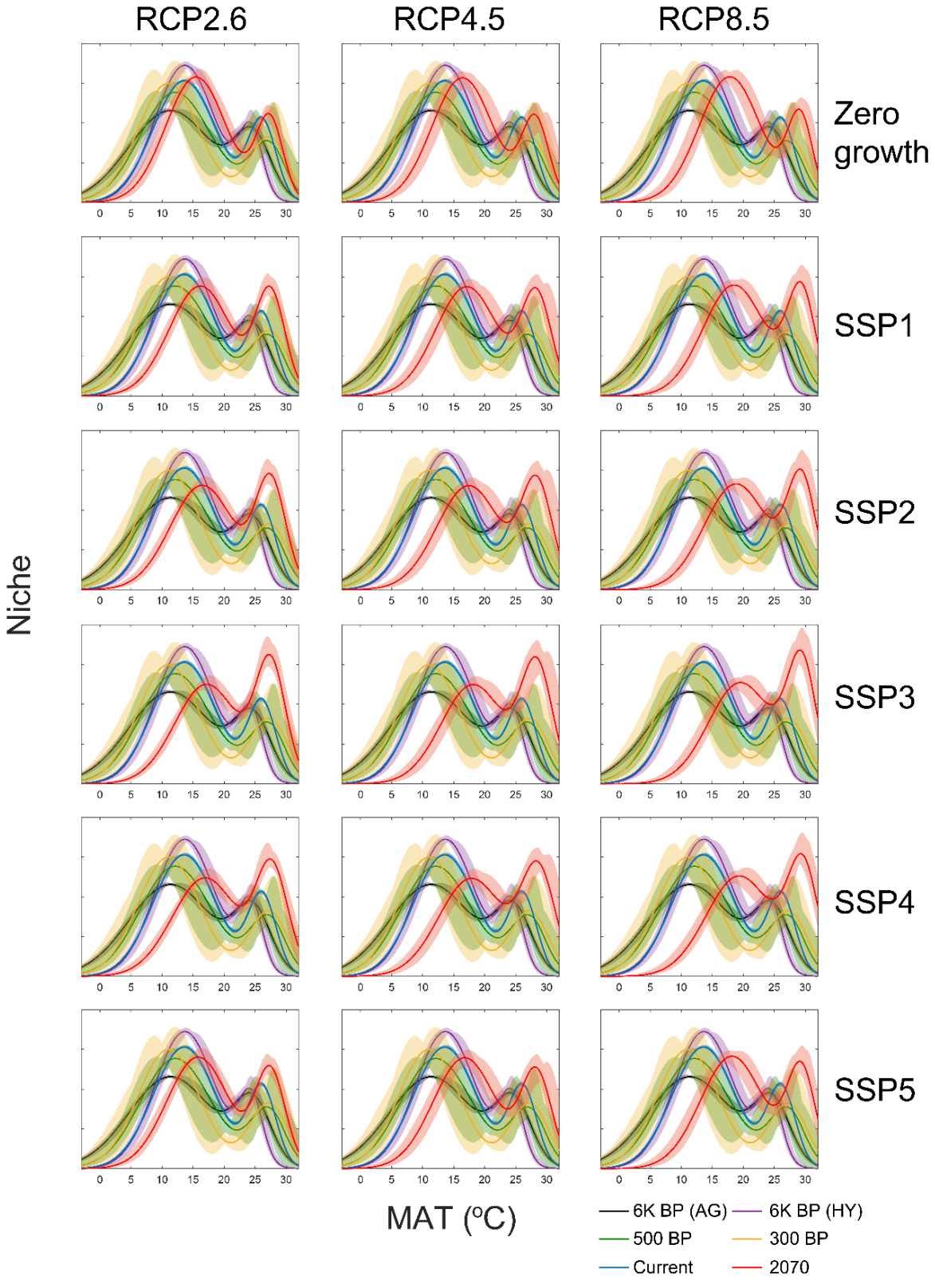

Figure S8. Geographical hotspots of the modeled human temperature niche are similar between 6Ky BP and current conditions. The niche was fitted by double Gaussian models based on the past population and climate conditions, using the gray (panel A, based on reconstructed ArchaeoGlobe population data), purple (panel B, based on reconstructed HYDE population data), and blue (panel C, projecting the current niche to the past climate, assuming that the niche would remain unchanged) curves in Fig. S7. The current niche map in Fig. 4A is also shown in panel D for comparison. The areas outside 90 (black hatched), 95 (blue hatched) and 99 (red hatched) percentiles of suitability are shown.

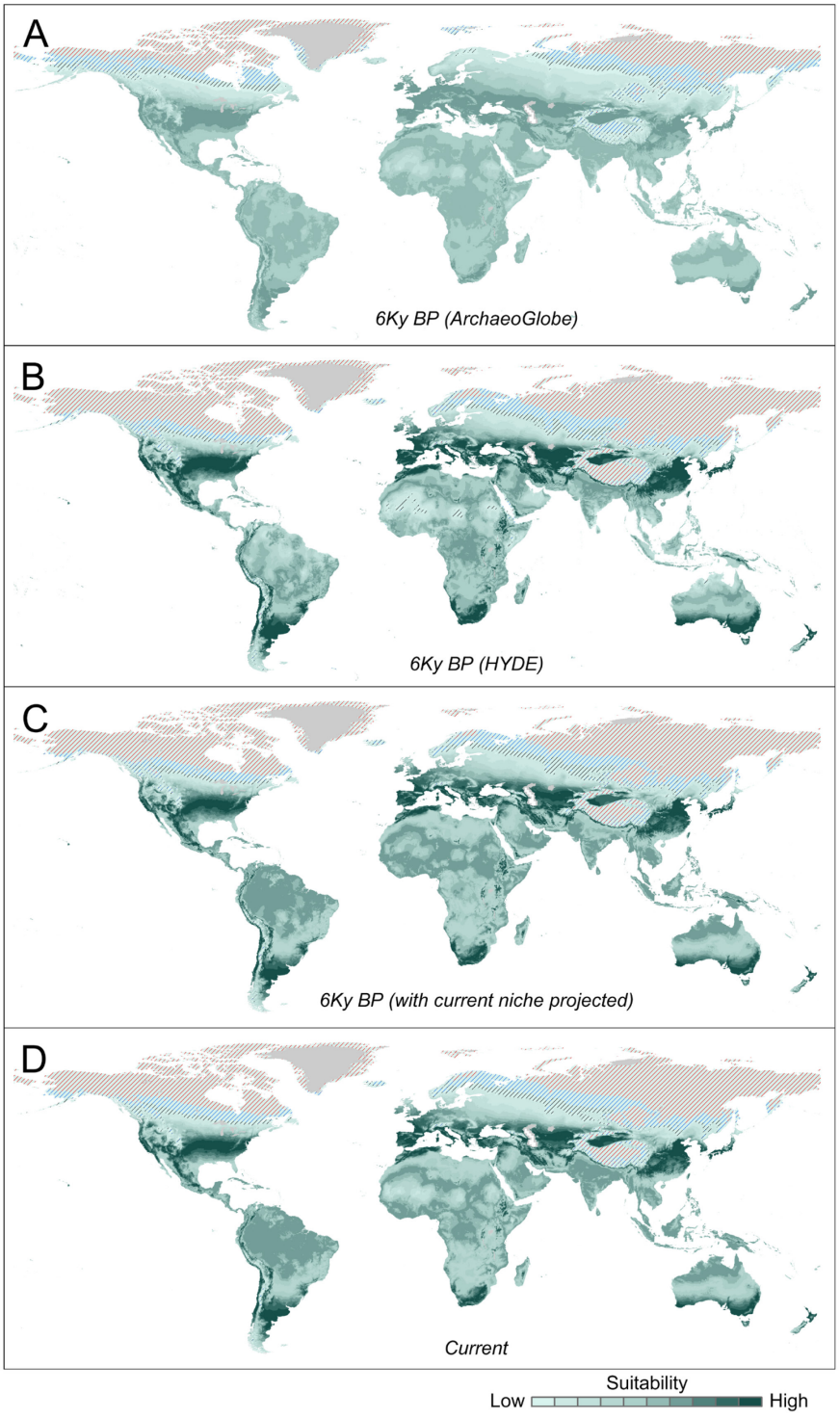

Figure S9. The geographical position (left column) and displacement (right column) of the human temperature niche projected on the past (6Ky BP) and 2070 climate (under RCP 2.6, RCP 4.5 and RCP 8.5, respectively). The maps in the left column represent relative human distributions (summed to unity) for the imaginary situation that humans would be distributed over temperatures following the stylized double Gaussian model fitted to the modern data (the blue dashed curve in Fig. 2A). The areas outside 90 (black hatched), 95 (blue hatched) and 99 (red hatched) percentiles of suitability are shown. The maps in the right column represent geographic displacement of the human niche relative to the current situation (+: gain, -: loss). Note that the 6Ky BP map (same as Fig. S8C) is generated by projecting the modern human climate niche to the past climate, assuming the human niche would remain unchanged over time.

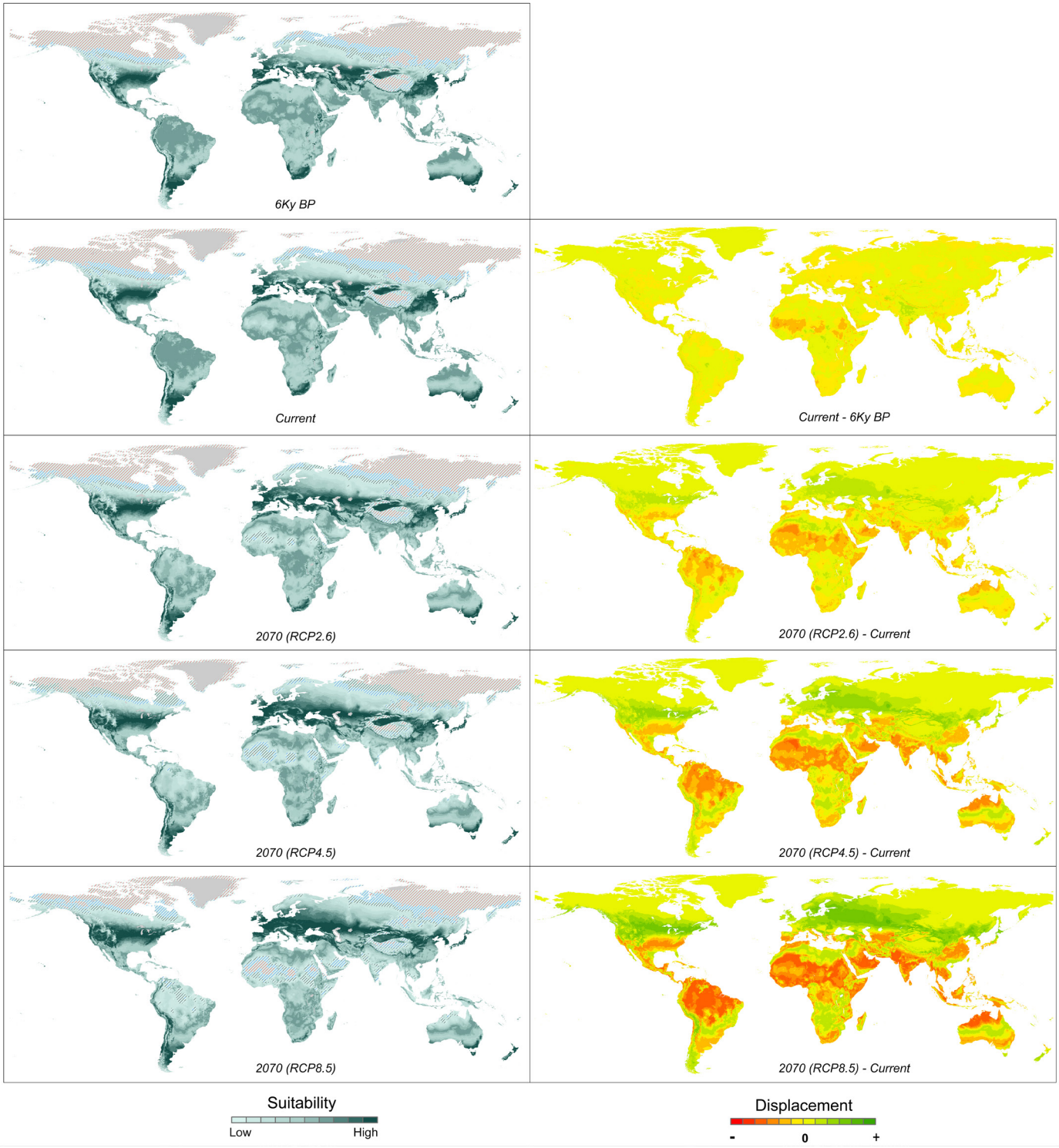

Figure S10. The geographical position (left column) and displacement (right column) of the human niche (relative to available combinations of mean annual temperature and precipitation) projected on the past (6Ky BP) and 2070 climate (under RCP 2.6, RCP 4.5 and RCP 8.5, respectively). The maps in the left column represent relative human distributions (summed to unity) for the imaginary situation that humans would be distributed following the current conditions of mean annual temperature and precipitation (the smoothed surface in Fig. 1A). The areas outside 90 (black hatched), 95 (blue hatched) and 99 (red hatched) percentiles of suitability are shown. The maps in the right column represent geographic displacement of the human niche relative to the current situation (+: gain, -: loss). Note that the 6Ky BP map is generated by projecting the modern human climate niche to the past climate, assuming the human niche would remain unchanged over time.

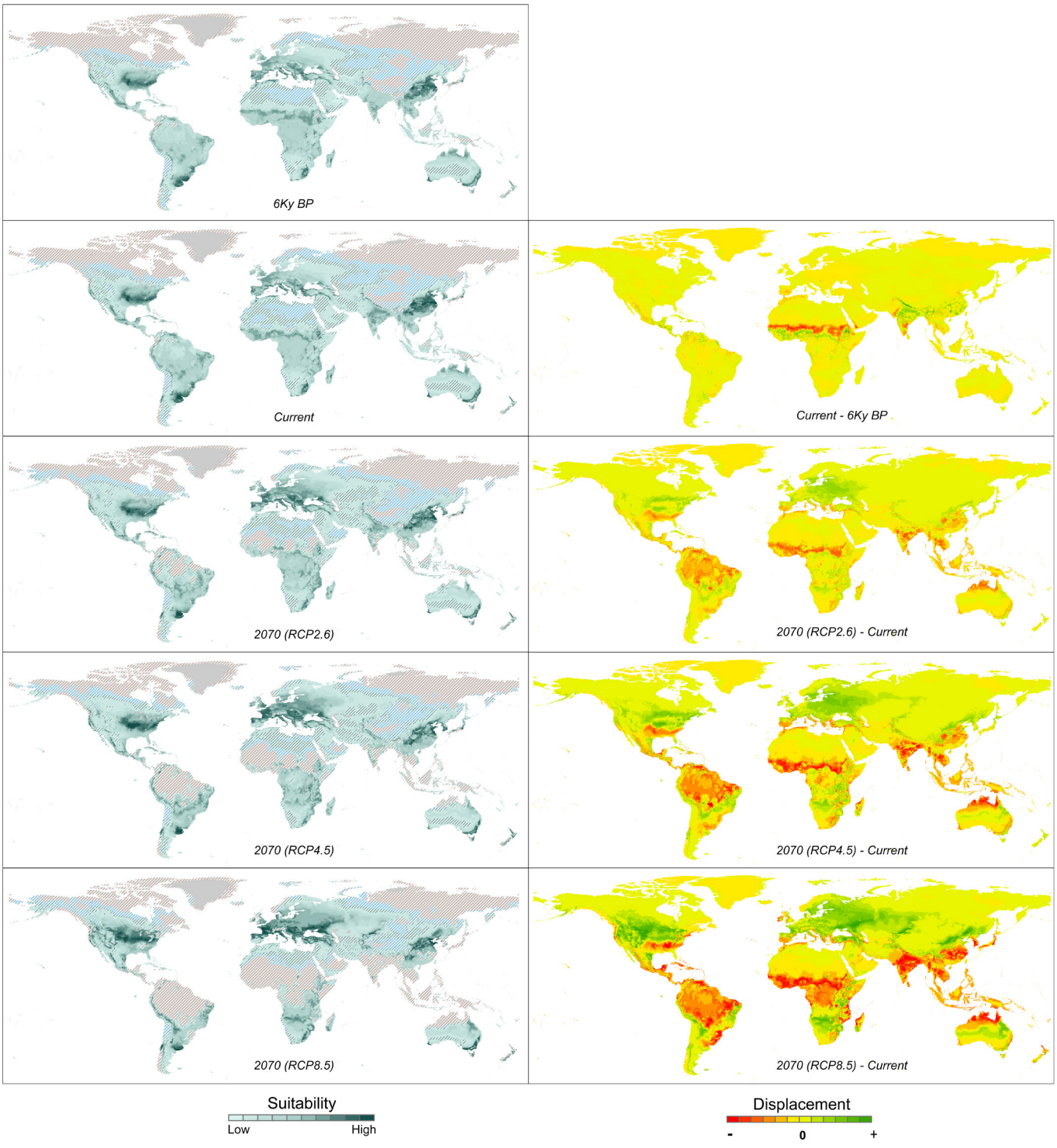

Figure S11. Mean absolute geographic latitude of realized human climate niche in the past ~6000 years (from mid-Holocene), current and the future ~50 years (by the year 2070, if we were to keep the same climate niche, i.e., the distribution relative to mean annual temperature depicted in Fig. 2A). Boxplots and data points (gray dots) are shown for the ensemble of climate models (and 2 population datasets for the current conditions). For 6Ky BP, we reconstructed the niche using the ArchaeoGlobe (the AG box) and the HYDE (the HY box) population data using the gray and purple curves in Fig. S7, respectively; we also projected the modern human niche (the blue curves in Fig. S7) to the past climate (the PMNP box), assuming the human niche would remain unchanged over time.

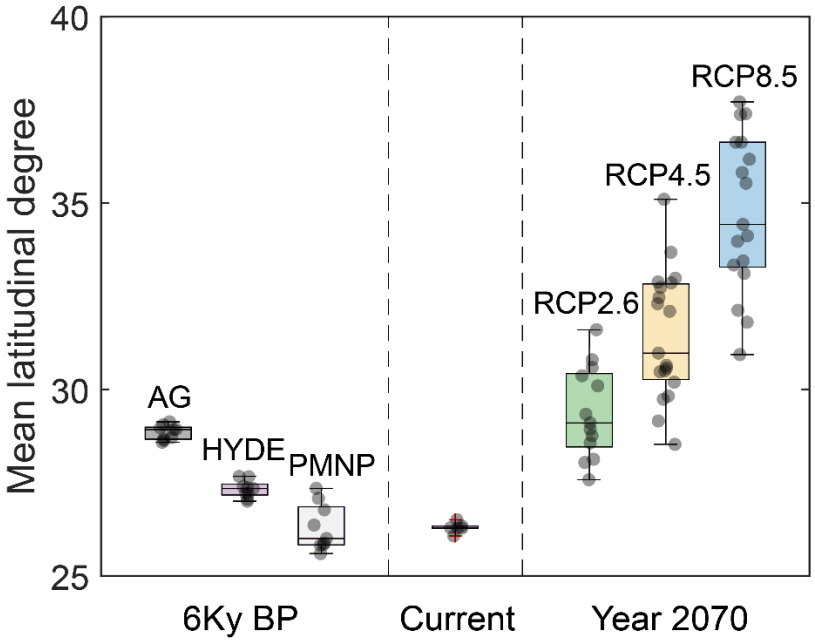

Figure S12. Estimated percentage geographical displacement of human climate niche in the past ~6000 years (since mid-Holocene) and the future ~50 years (by the year 2070 under different RCPs, if we were to keep the same climate niche, i.e., the distribution relative to mean annual temperature depicted in Fig. 2A). Boxplots and data points (gray dots) are shown for the ensemble of climate models. For 6Ky BP, we reconstructed the niche using the ArchaeoGlobe (the AG box) and the HYDE (the HY box) population data using the gray and purple curves in Fig. S7, respectively; we also projected the modern human niche (the blue curves in Fig. S7) to the past climate (the PMNP box), assuming the human niche would remain unchanged over time.

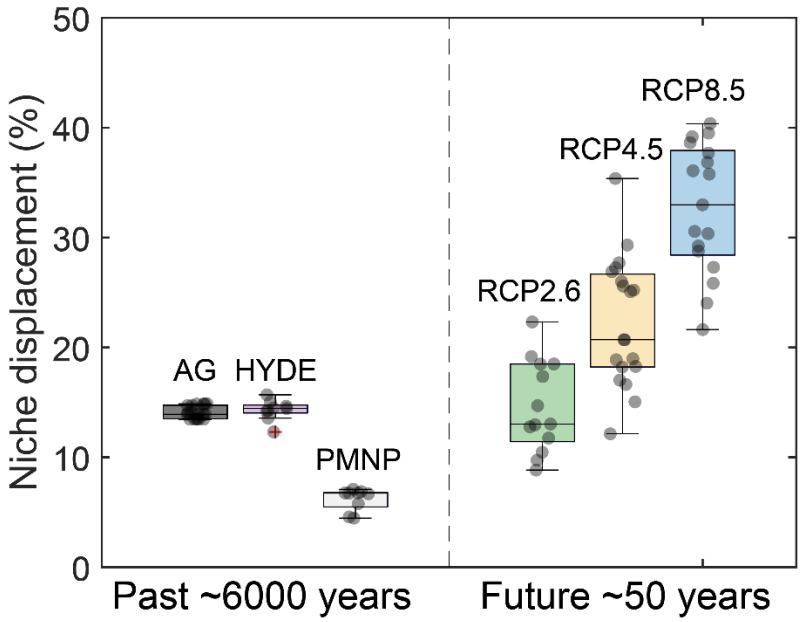

Figure S13. Number of people who would need to be displaced in different demographic and climate scenarios if we were to keep the same climate niche (the distribution relative to mean annual temperature depicted in Fig. 2A) in the future ~ 50 years. Boxplots and data points (gray dots) are shown for the ensemble of climate models.

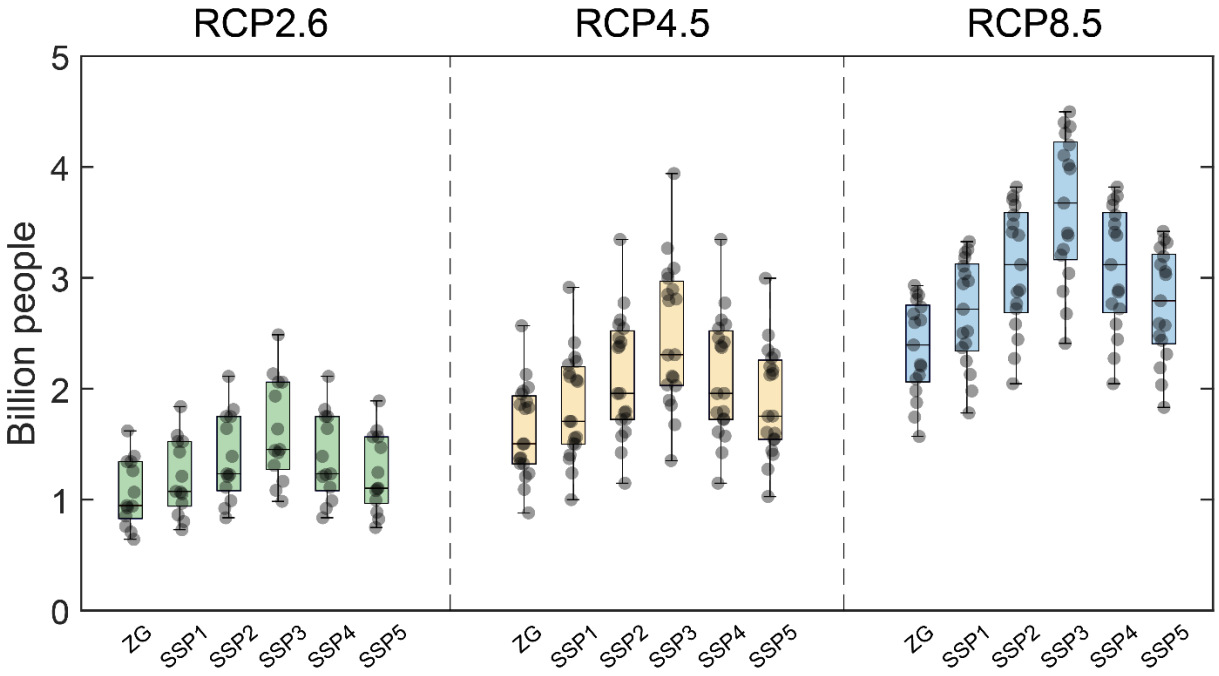

Table S3. World population and temperature rise (relative to the pre-industrial baseline) projected by different demographic and climate scenarios around the year 2070, and number (mean ± std for the ensemble of climate models) of people who would need to be displaced in different demographic and climate scenarios if we were to keep the same climate niche (the distribution relative to mean annual temperature depicted by the blue dashed curve in Fig. 2A).

Demographic scenario (Shared Socio-economic Pathways, SSPs)	**World population growth (billion)**	**World population size (billion)**	**Climate scenario**		
			RCP 2.6	**RCP 4.5**	**RCP 8.5**
			mean projected global temperature rise of ~1.5 °C	-	mean projected global temperature rise of ~3.2 °C
			Displaced people (billion)	**Displaced people (billion)**	**Displaced people (billion)**
Zero growth	0.00	7.26	1.06±0.30	1.62±0.42	2.37±0.43
SSP1	0.98	8.24	1.20±0.34	1.84±0.48	2.69±0.49
SSP2	2.20	9.46	1.38±0.39	2.12±0.55	3.09±0.56
SSP3	3.88	11.14	1.63±0.46	2.49±0.65	3.64±0.66
SSP4	2.20	9.46	1.38±0.39	2.12±0.55	3.09±0.56
SSP5	1.21	8.47	1.24±0.35	1.89±0.49	2.76±0.50

Figure S14. Number of people who would need to be displaced by the year 2070 per Celsius degree warming relative to the pre-industrial period in different demographic and climate scenarios if we were to keep the same climate niche (the distribution relative to mean annual temperature depicted by the blue dashed curve in Fig. 2A). Boxplots and data points (gray dots) are shown for the ensemble of climate models.

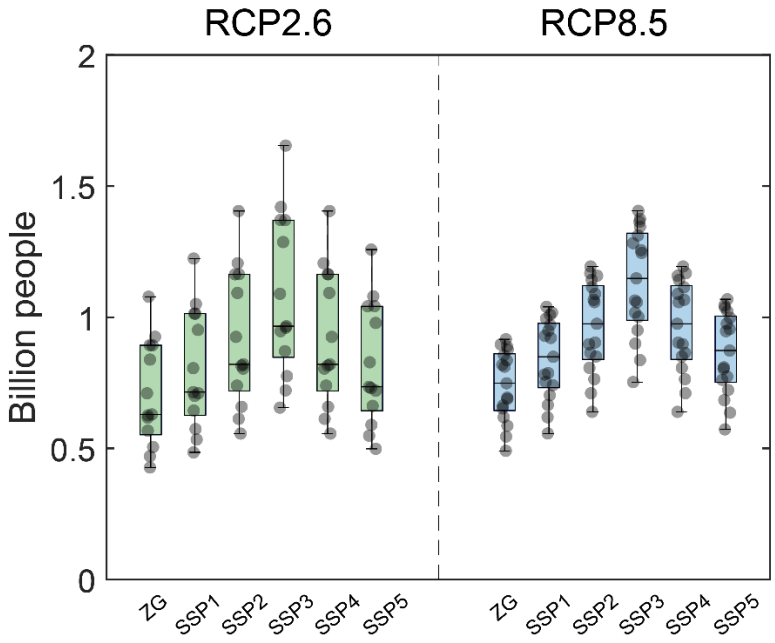

References

1 Klein Goldewijk, K., Beusen, A. & Janssen, P. Long-term dynamic modeling of global population and built-up area in a spatially explicit way: HYDE 3.1. *The Holocene* **20**, 565-573 (2010).

2 Chaput, M. A. & Gajewski, K. Radiocarbon dates as estimates of ancient human population size. *Anthropocene* **15**, 3-12 (2016).

3 Fuller, D. Q. *et al.* The contribution of rice agriculture and livestock pastoralism to prehistoric methane levels: An archaeological assessment. *The Holocene* **21**, 743-759 (2011).

4 Stephens, L. *ArchaeoGLOBE Public Data*. (Harvard Dataverse, 2019).

5 Stephens, L. *ArchaeoGLOBE Regions*. (Harvard Dataverse, 2018).

6 Binford, L. R. *Constructing Frames of Reference: An Analytical Method for Archaeological Theory Building Using Hunter-Gatherer and Environmental Data Sets*. (University of California Press, 2001).

7 Hassan, F. A. *Demographic Archaeology*. (New York: Academic Press, 1981).

8 Jones, B. & O'Neill, B. Spatially explicit global population scenarios consistent with the Shared Socioeconomic Pathways. *Environmental Research Letters* **11**, 084003 (2016).

9 Kummu, M., Taka, M. & Guillaume, J. H. Gridded global datasets for Gross Domestic Product and Human Development Index over 1990–2015. *Scientific Data* **5**, 180004 (2018).

10 Kummu, M., Taka, M. & Guillaume, J. H. A. (Dryad Data Repository, 2018).

11 FAO/IIASA. *Global Agro-ecological Zones (GAEZ v3.0)*. (2011).

12 Robinson, T. P. *et al.* Mapping the global distribution of livestock. *PloS One* **9**, e96084 (2014).

13 Hijmans, R. J., Cameron, S. E., Parra, J. L., Jones, P. G. & Jarvis, A. Very high resolution interpolated climate surfaces for global land areas. *International Journal of Climatology* **25**, 1965-1978 (2005).

14 Braconnot, P. *et al.* Evaluation of climate models using palaeoclimatic data. *Nature Climate Change* **2**, 417-424 (2012).

15 Huston, M. A. Precipitation, soils, NPP, and biodiversity: resurrection of Albrecht's curve. *Ecol Monogr* **82**, 277-296 (2012).

16 FAO/IIASA/ISRIC/ISSCAS/JRC. Harmonized world soil database (version 1.2). *FAO, Rome, Italy and IIASA, Laxenburg, Austria* (2012).

17 Center for International Earth Science Information Network (CIESIN)—Columbia University. Gridded population of the world, version 4 (GPWv4): population density (2016).

18 Mitchell, T. D. & Jones, P. D. An improved method of constructing a database of monthly climate observations and associated high-resolution grids. *International Journal of Climatology* **25**, 693-712 (2005).

19 Abatzoglou, J. T., Dobrowski, S. Z., Parks, S. A. & Hegewisch, K. C. TerraClimate, a high-resolution global dataset of monthly climate and climatic water balance from 1958–2015. *Scientific Data* **5**, 170191 (2018).

20 Meinshausen, M. *et al.* The RCP greenhouse gas concentrations and their extensions from 1765 to 2300. *Climatic Change* **109**, 213 (2011).

21 Phipps, S. *et al.* The CSIRO Mk3L climate system model version 1.0–Part 2: Response to external forcings. *Geoscientific Model Development* **5**, 649-682 (2012).

22 Schmidt, G. A. *et al.* Configuration and assessment of the GISS ModelE2 contributions to the CMIP5 archive. *Journal of Advances in Modeling Earth Systems* **6**, 141-184 (2014).

23 Gordon, C. *et al.* The simulation of SST, sea ice extents and ocean heat transports in a version of the Hadley Centre coupled model without flux adjustments. *Climate Dynamics* **16**, 147-168 (2000).

24 Dufresne, J.-L. *et al.* Climate change projections using the IPSL-CM5 Earth System Model: from CMIP3 to CMIP5. *Climate Dynamics* **40**, 2123-2165 (2013).

25 Stevens, B. *et al.* Atmospheric component of the MPI-M Earth system model: ECHAM6. *Journal of Advances in Modeling Earth Systems* **5**, 146-172 (2013).